ORNL/TM-2022/1841

Impacts of LEU+ and HBU Fuel on Decay Heat and Radiation Source Term

Nicholas Kucinski
Peter Stefanovic
Justin Clarity
William Wieselquist

April 2022

OAK RIDGE National Laboratory

ORNL IS MANAGED BY UT-BATTELLE LLC FOR THE US DEPARTMENT OF ENERGY

ORNL/TM-2022/1841

Nuclear Energy and Fuel Cycle Division

IMPACTS OF LEU+ AND HBU FUEL ON DECAY HEAT AND RADIATION SOURCE TERM

Nicholas Kucinski
Peter Stefanovic
Justin Clarity
William Wieselquist

April 2022

Prepared by
OAK RIDGE NATIONAL LABORATORY
Oak Ridge, TN 37831-6283
managed by
UT-BATTELLE LLC
for the
US DEPARTMENT OF ENERGY
under contract DE-AC05-00OR22725

CONTENTS

LIST OF TABLES

LIST OF FIGURES

ABBREVIATIONS

BWR	boiling water reactor
IFBA	integral fuel burnable absorber
LEU	low-enriched uranium
LWR	light water reactor
MAVRIC	Monaco with Automated Variance Reduction Using Importance Calculations
ORIGEN	Oak Ridge Isotope Generation
PCT	peak cladding temperature
PWR	pressurized water reactor
SFP	spent fuel pool
SNF	spent nuclear fuel
UNF-ST&DARDS	Used Nuclear Fuel—Storage, Transportation & Disposal Analysis Resource and Data System
W 17 × 17 STD	Westinghouse 17 × 17 Standard
WABA	wet annular burnable absorber

ABSTRACT

Using low-enriched uranium with ^{235}U enrichment slightly greater than 5.0 wt % (LEU+) fuel is desirable for light water reactors (LWR) because it can enable longer cycles and/or smaller fresh fuel batches. This report analyzes the impact of LEU+ on back-end considerations, such as its impact on the spent fuel pool, and on the thermal and shielding performance of dry storage systems. For both pressurized water reactor (PWR) and boiling water reactor LEU+ fuel, this report concludes that additional cooling time or regionalized loading plans are required to maintain the same level of thermal and shielding performance of dry storage systems loaded with LEU fuel. For PWR fuel, this report concludes that the impact of LEU+ fuel on the time-to-boil of a spent fuel pool (SFP) is minimal and does not require considerable changes in SFP management.

1. INTRODUCTION

This report documents a quantitative analysis that investigated the effect of loading low-enriched uranium (LEU) plus (LEU+) fuel with increased burnup on the thermal and shielding performance of current dry storage cask systems. Peak cladding temperature (PCT) and cask dose rates were calculated for standard LEU fuel and LEU+ fuel cases. PCT is an important parameter in dry storage, and limitations on PCT were imposed to maintain fuel and cladding integrity and prevent hydride reorientation. Nuclide contributions to decay heat were analyzed for both LEU and LEU+ fuel. The impact of the integral fuel burnable absorber (IFBA) amount and configuration in LEU and LEU+ fuel on thermal and shielding performance of dry storage casks was analyzed for PWR fuel by analyzing multiple absorber layouts. The additional amount of time in wet storage required for LEU+ fuel to result in no increase in PCT or dose rates compared with baseline LEU values was calculated. The impact of LEU+ on spent fuel pool (SFP) management was also investigated by calculating the time-to-boil for an SFP loaded with LEU or LEU+ fuel.

Spent fuel source term generation, decay, and shielding calculations were performed using the SCALE [1] sequences Polaris, ORIGAMI, and Monaco with Automated Variance Reduction Using Importance Calculations (MAVRIC). PCT was calculated by using COBRA-SFS [2]. Source terms, shielding, and PCT calculations were performed using the Used Nuclear Fuel—Storage, Transportation & Disposal Analysis Resource and Data System (UNF-ST&DARDS) tool [3].

2. CODES AND MODELS

This section briefly describes the codes used in this work.

2.1 SCALE

The SCALE code system is a widely used modeling and simulation suite for nuclear safety analysis and design that is developed, maintained, tested, and managed by the Nuclear Energy and Fuel Cycle Division of Oak Ridge National Laboratory [1]. SCALE provides a comprehensive, verified, and validated user-friendly tool set for criticality safety, reactor physics, radiation shielding, radioactive source term characterization, and sensitivity and uncertainty analysis.

2.1.1 Polaris

Polaris provides a 2D lattice physics analysis capability for light water reactors (LWRs). Polaris uses a transport solver based on the method of characteristics and a multigroup self-shielding method called the

embedded self-shielding method. Polaris is integrated with the Oak Ridge Isotope Generation (ORIGEN) module of SCALE for depletion calculations.

2.1.2 ORIGEN/ORIGAMI

The ORIGEN module of SCALE calculates time-dependent concentrations, activities, and radiation source terms for many isotopes simultaneously generated or depleted by neutron transmutation, fission, and decay. ORIGEN is used internally within Polaris to perform depletion and decay. It can also be used to perform stand-alone decay calculations on nuclide inventories generated by Polaris. ORIGAMI computes detailed isotopic compositions for LWR assemblies.

2.1.3 MAVRIC

The MAVRIC fixed-source radiation transport sequence of SCALE is designed to apply the multigroup and continuous-energy fixed-source Monte Carlo code, Monaco, to calculate fluxes and dose rates with low uncertainties in reasonable times, even for deep-penetration problems.

2.2 COBRA-SFS

COBRA-SFS is the primary thermal analysis tool within UNF-ST&DARDS. It is used to perform thermal-hydraulic analyses of multi-assembly spent nuclear fuel (SNF) storage and transportation systems at fuel rod-level detail [2]. The code is developed and maintained by Pacific Northwest National Laboratory, and it has been validated against measured data for analyzing spent fuel storage systems [4].

COBRA-SFS templates were developed for cask systems and are coupled with the cask loading data to perform thermal analyses in UNF-ST&DARDS. These thermal models were used to calculate the PCT and the temperature distributions throughout the system for components of interest. Assembly-specific decay heat loads and burnup-dependent axial profiles were calculated via nuclear analysis with UNF-ST&DARDS and used as an input to COBRA-SFS. The thermal models were used to determine the time-dependent temperature histories based on the assumed environmental variables.

COBRA-SFS uses a stand-alone utility, RADGEN [5], to generate gray-body view factors for the thermal radiation calculations. The gray-body view factors were used to determine thermal radiation heat transfer in the assembly, the fuel rod region, and other cavities via the COBRA-SFS code. In future releases of COBRA-SFS, the RADGEN utility will be integrated within the main code.

To automate the generation of assembly inputs provided to the COBRA-SFS templates and to automate the generation of the input required by RADGEN, a COBRA-COMANDER (Creator of Most Assemblies' Necessary Data, Even RADGEN) utility was integrated into the UNF-ST&DARDS tool.

2.3 UNF-ST&DARDS

The UNF-ST&DARDS is an automated, comprehensive data and analysis tool [3]. UNF-ST&DARDS provides a unified SNF database integrated with nuclear analysis codes, such as SCALE and COBRA-SFS, to streamline SNF and related systems characterizations. UNF-ST&DARDS capabilities and architecture have been discussed in detail in other works. The unified database within the UNF-ST&DARDS enables assembly-specific depletion and decay, as well as cask-specific criticality, dose, containment, and thermal analyses.

2.4 MAVRIC DRY STORAGE CASK MODELS

2.4.1 GENERAL-37

The General-37 MAVRIC model developed for shielding analysis with UNF-ST&DARDS was used in this work. This cask model is intended to be a generic, nonproprietary model used to calculate total dose rates on the surface and at 1 m from the cask surface. The basket can hold 37 PWR fuel assemblies. The assembly type modeled is the Westinghouse 17 × 17 Standard (W 17 × 17 STD) design, which has 25 fuel rod locations displaced by instrument and guide tubes. Each fuel pin is explicitly modeled, and the active fuel region is separated into 18 axial zones to accommodate axially varying burnup profiles. ANSI Standard (1977) [6] flux-to-dose rate conversion factors are used to calculate dose rates in millirems per hour. An *X-Y* view of the fuel region of the model is provided in Figure 1, and an *X-Z* view of the fuel region is provided in Figure 2. The surface tally volume used in this analysis is identified on each figure. Select component materials are provided in Table 1, and dimensions are provided in Table 2.

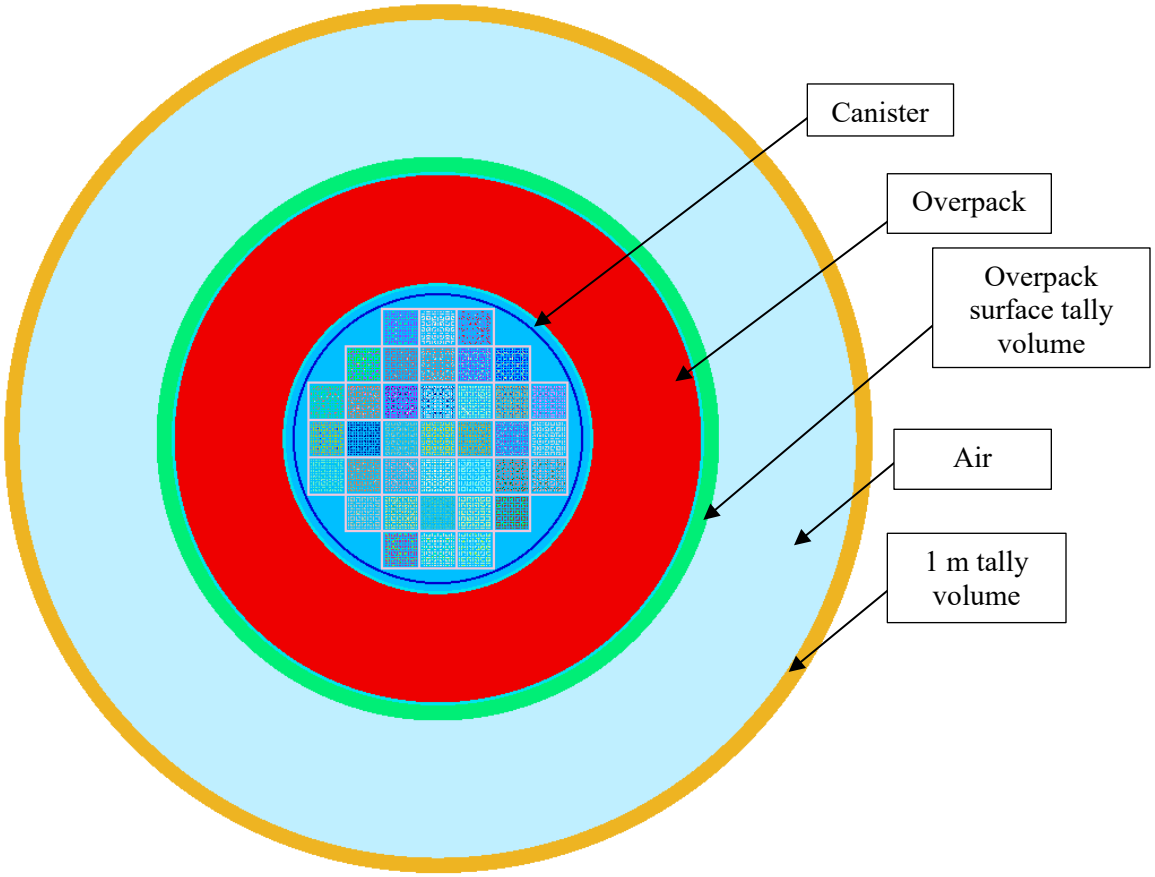

Figure 1. *X-Y* view of General-37 MAVRIC shielding model.

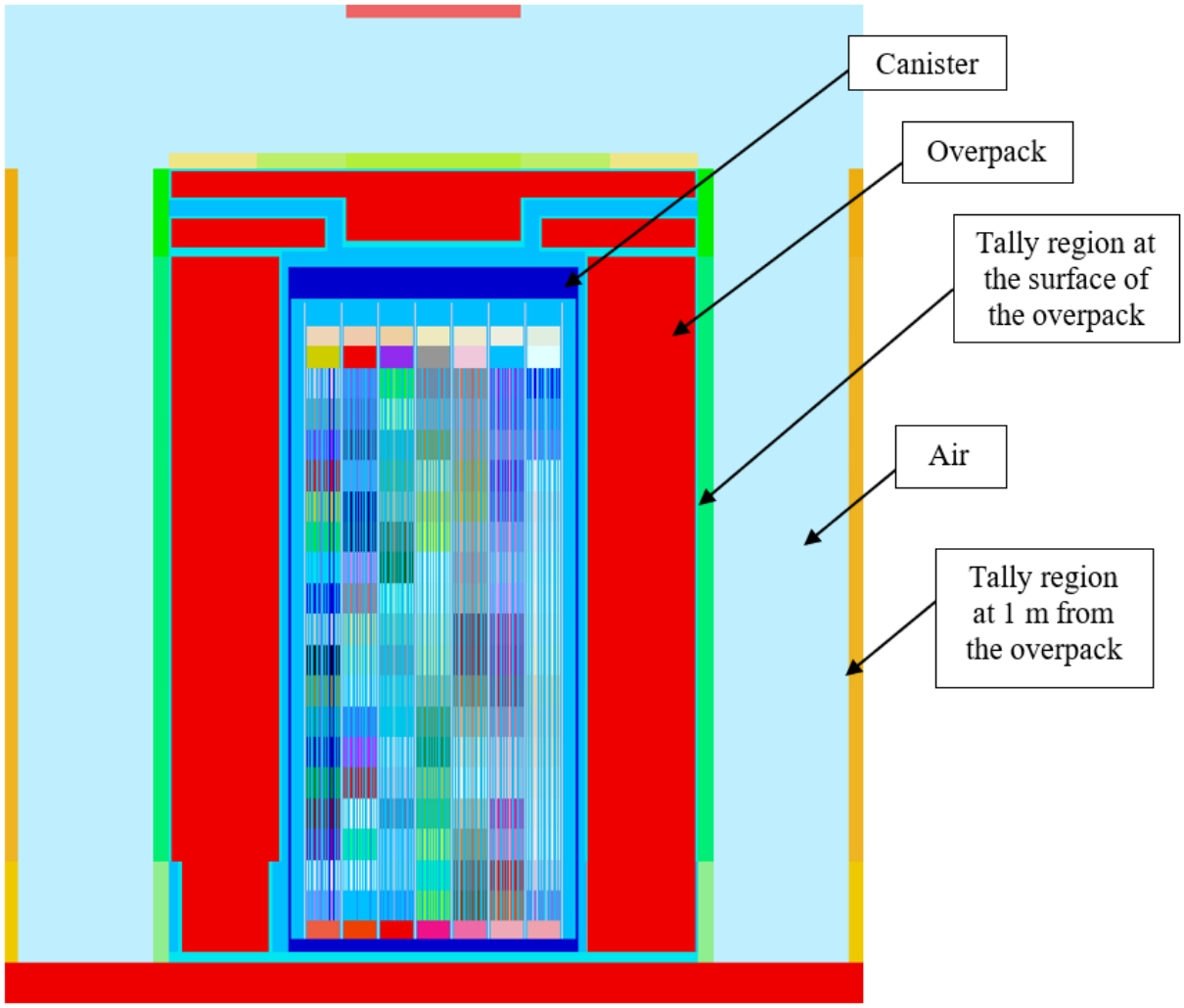

Figure 2. *X-Z* view of General-37 MAVRIC shielding model.

Table 1. General-37 MAVRIC model component materials.

Component	Material
Canister	Stainless steel
Basket	Borated aluminum
Overpack structure	Carbon steel
Overpack shielding material	Concrete

Table 2. General-37 MAVRIC model dimensions.

Parameter	Value (cm)
Canister outer radius	95.5
Cannister shell thickness	1.5
Canister overall height	453
Overpack inner radius	100
Overpack outer radius	175
Overpack overall height	525

2.4.2 GENERAL-89

The General-89 MAVRIC model developed for shielding analysis with UNF-ST&DARDS was used for boiling water reactor (BWR) analysis in this work. This cask model is intended to be a generic, nonproprietary model used to calculate total dose rates on the surface and at 1 m from the cask surface. The basket can hold 89 boiling water reactor (BWR) fuel assemblies. The assembly type modeled is the GE-14 10 × 10 design, which has 92 fuel rods and two water rods that each occupy four locations. Each fuel pin is explicitly modeled, and the active fuel region is separated into 10 axial nodes to accommodate axially varying burnup profiles. ANSI Standard (1977) [6] flux-to-dose rate conversion factors are used to calculate dose rates in millirems per hour. An *X-Y* view of the fuel region of the model is provided in Figure 3, and an *X-Z* view of the fuel region is provided in Figure 4. The surface tally volume used in this analysis is identified on each figure. Select component materials are provided in Table 3, and dimensions are provided in Table 4.

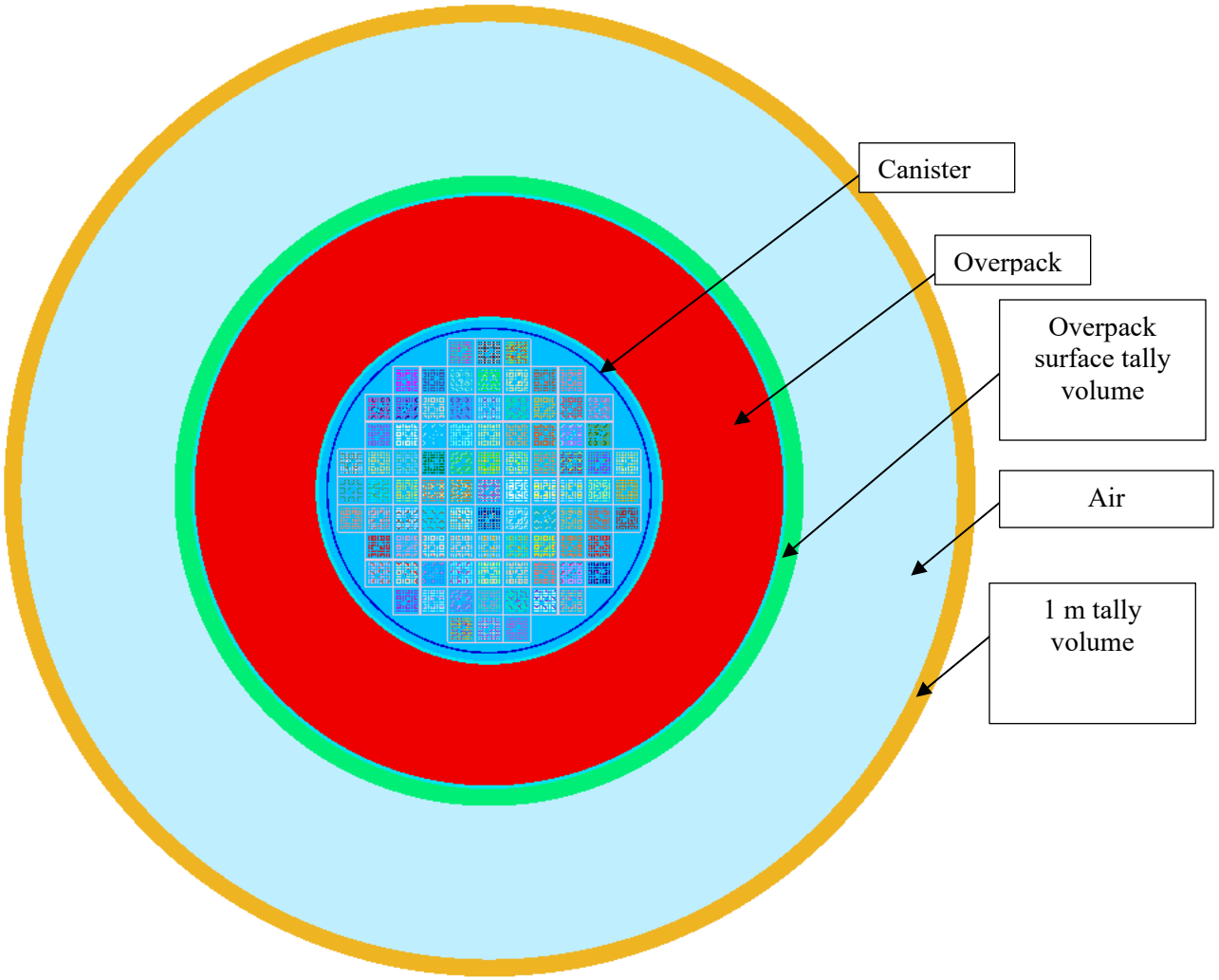

Figure 3. *X-Y* view of General-89 MAVRIC shielding model.

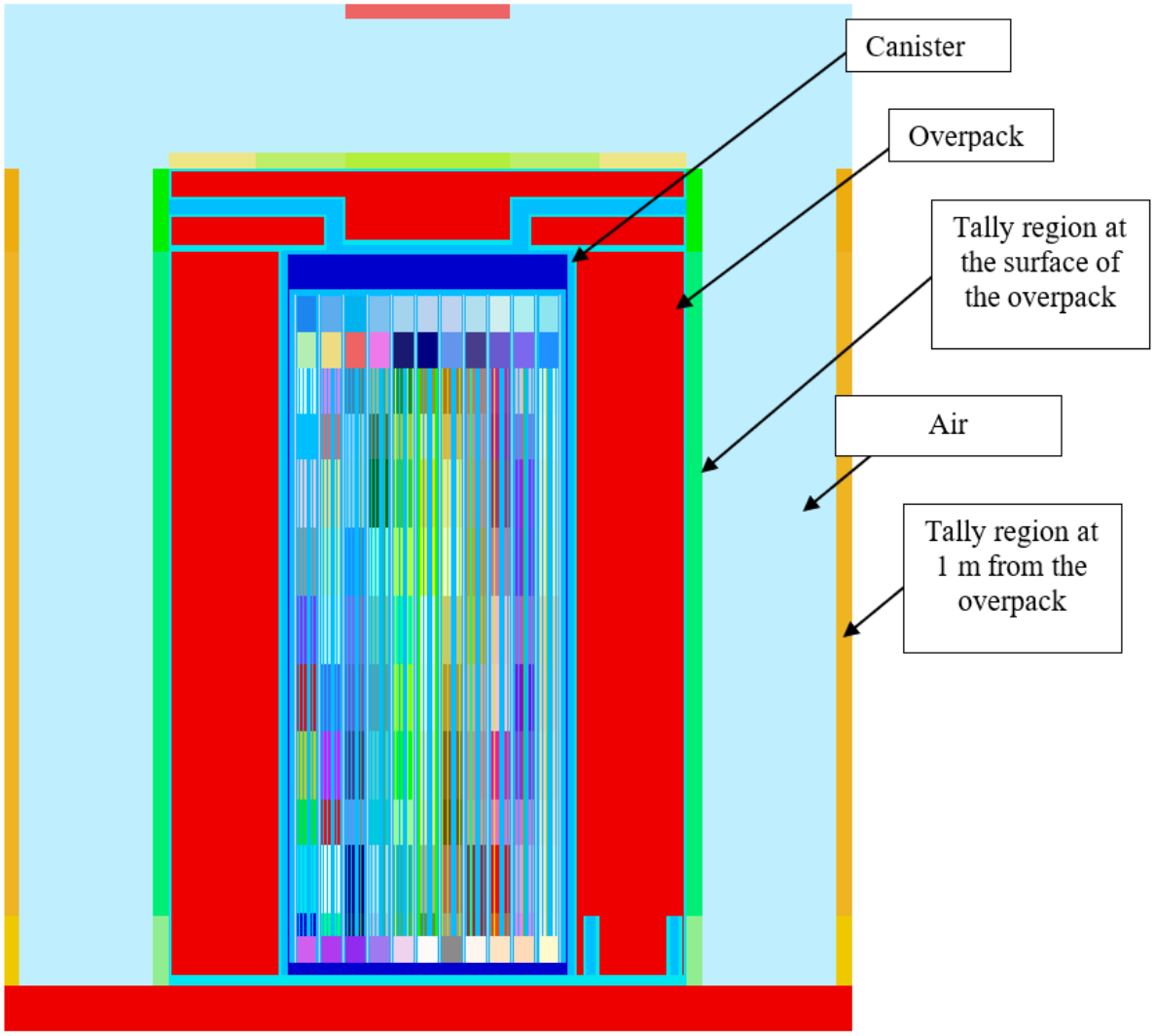

Figure 4. X-Z view of General-89 MAVRIC shielding model.

Table 3. General-89 MAVRIC model component materials.

Component	Material
Canister	Stainless steel
Basket	Borated aluminum
Overpack structure	Carbon steel
Overpack shielding material	Concrete

Table 4. General-89 MAVRIC model dimensions.

Parameter	Value (cm)
Canister outer radius	95.7
Cannister shell thickness	1.2
Canister overall height	483
Overpack inner radius	100
Overpack outer radius	175
Overpack overall height	525

2.5 COBRA-SFS DRY STORAGE CASK MODELS

2.5.1 GENERAL-37

The General-37 COBRA-SFS model developed for thermal analysis with UNF-ST&DARDS was used in this work. This cask model is intended to be a generic, nonproprietary model used to calculate PCT and temperature distributions throughout the materials in the cask.

The model comprises a fuel basket inside a sealed stainless-steel canister, which is surrounded by a concrete overpack. There is an annular region between the canister and overpack through which air flows. The model has an upper plenum region, a fuel basket region, and a lower plenum. These plenum regions are modeled as 1D arrays of materials through which conduction heat transfer to the environment is modeled. The upper plenum region starts at the gas space above the fuel region and includes the stainless-steel lid of the canister, the gas plenum between the canister and overpack lids, and the overpack lid. The lower plenum starts at the gas space below the fuel region and includes the base of the canister and the overpack baseplate. The basket region is divided into 47 axial nodes to capture the temperature variation along the height of the container.

In the model, the inlet and outlet for each subchannel of each assembly are connected to a common upper and lower plenum to allow natural recirculation flow within the canister to be directly calculated by using the fluid mass, momentum, and energy conservation equations. Momentum losses are modeled with wall friction factors, and they form drag loss coefficients for impediments in the flow field, such as grid spacers, tie plates, and assembly inlet/exit nozzles. To enable convective heat transfer, fluid channels are thermally connected to the fuel rods and the surrounding solid conduction nodes representing the basket by means of a user-specified heat transfer correlation. The fluid energy equation includes conduction through the fluid (i.e., He gas) in the subchannels, but the gas is assumed to be transparent to thermal radiation. Thermal radiation within the basket is calculated via 2D (i.e., planar cross section) gray-body view factors for the rod array and the surrounding solid conduction nodes of the basket wall.

The basket can hold 37 PWR fuel assemblies. The assembly type modeled is the W 17 × 17 STD design, which has 25 fuel rod locations displaced by instrument and guide tubes. Each fuel pin was explicitly modeled. Assembly-specific decay heat load–applying burnup-dependent axial profiles were calculated in SCALE and used as input to the COBRA-SFS model. The COBRA-SFS model is full geometry (i.e., no symmetry) to accommodate realistic, potentially asymmetric geometries or fuel loading patterns.

2.5.2 GENERAL-68

Because of the availability of existing models, thermal analysis for the BWR canister was performed by using a General-68 COBRA-SFS model. The General-68 COBRA-SFS model developed for thermal analysis with UNF-ST&DARDS was used in this work. This cask model is intended to be a generic, nonproprietary model used to calculate PCT and temperature distributions throughout the materials in the cask. The general description of the model is identical to the General-37 COBRA-SFS model.

The basket can hold 68 BWR fuel assemblies. The assembly type modeled is the GE-14 10 × 10 design, which has 92 fuel rods and two water rods that each occupy four lattice locations. Each fuel pin is explicitly modeled. Assembly-specific decay heat load–applying burnup-dependent axial profiles were calculated in SCALE and used as input to the COBRA-SFS model. The COBRA-SFS model is full geometry (i.e., no symmetry) to accommodate realistic, potentially asymmetric geometries or fuel loading patterns.

2.6 TIME-TO-BOIL METHODOLOGY

The time-to-boil of the water in an SFP (h) after the loss of forced cooling is calculated by the following equation:

$$\tau_{boil} = \frac{C}{Q_{GEN}}(212°\text{F} - T) \quad (1)$$

where C is the SFP water thermal capacity (Btu/°F), Q_{GEN} is the heat generation rate in the SFP (Btu/h), and T is the SFP bulk water temperature (°F).

The time-to-boil was calculated by multiplying the heat-up rate of the water by the difference of the boiling temperature of water and the SFP bulk water temperature at the time of the forced cooling loss. The derivation of this equation is described in further detail in Abella, Kawata, and Onoue [7]. In this analysis, the Q_{GEN} term was calculated by performing ORIGAMI discharge and decay calculations for each assembly in the SFP. The SFP water thermal capacity and the bulk water temperature at the time of forced cooling loss were assumed to be constant.

3. ANALYSIS

This work examined the effects of the changes in fuel characteristics associated with the transition to LEU+ enrichments and the associated increases in burnup. To perform this assessment, calculations were performed for baseline cases representative of the present operation. A second set of calculations was then performed to assess the expectations of LEU+ fuel increased burnup. Table 5 shows the assumed plant operating parameters for the PWR, and Table 6 shows the assumed plant operating parameters for the BWR.

Table 5. PWR plant operating parameters [8].

Parameter	LEU Baseline (core avg. 4.4 wt %)	LEU+ (core avg. 6.0 wt %)
Plant rating (MWe)	1,150	1,150
Plant rating (MWth)	3,626	3,626
Cycle length (months)	18	24
Cycle length (EFPD)	514	704
Number of assemblies in core	193	193
Fresh fuel enrichment (wt %)	4.2 / 4.6	5.95 / 6.2 / 6.6
Number of fuel batches	3	3
Fresh/once-burned/twice-burned at BOC	89 / 92 / 12	85 / 84 / 24
Number of assemblies discharged each cycle	92	84
Assembly average discharge burnup (GWd/MTU)	45.20	63.20
Max. assembly discharge burnup (GWd/MTU)	50.05	71.45
Max. nodal discharge burnup (GWd/MTU)	57.12	78.16
Core average burnup at EOC (GWd/MTU)	35.8	50.5
Average specific power (MW/MTU)	40.3	40.4
Cycle burnup accumulation (GWd/MTU)	24.8 / 18.4 / 8.1	34.3 / 27.6 / 10.4
Cycle-average specific power (MW/MTU)	48.3 / 35.8 / 15.8	48.8 / 39.2 / 14.8

Table 6. BWR plant operating parameters [9].

Parameter	LEU Baseline (assembly avg. 5.0 wt %)	LEU+ (assembly avg. 6.63 wt %)	LEU+ (assembly avg. 7.4 wt %)
Plant rating (MWe)	911	911	911
Plant rating (MWth)	2,804	2,804	2,804
Cycle length (months)	24	36	36
Cycle length (EFPD)	730.5	1,095.75	1,095.75
Number of assemblies in core	560	560	560
Fresh fuel enrichment (wt %)	5.0	6.63	7.4
Number of fuel batches	3	3	3
Fresh/once-burned/twice-burned at BOC	228 / 228 / 104	248 / 248 / 64	228 / 228 / 104
Number of assemblies discharged each cycle	0 / 124 / 104	0 / 184 / 64	0 / 124 / 104
Assembly average discharge burnup (GWd/MTU)	43.5	61.1	65.8
Max. assembly discharge burnup (GWd/MTU)	47.6 / 45.2 / 44.3	66.0 / 65.4 / 63.8	72.0 / 68.5 / 67.7
Max. nodal discharge burnup (GWd/MTU)	58.4	82.6	88.9
Core average burnup at EOC (GWd/MTU)	33.0	46.2	50.1
Average specific power (MW/MTU)	24.6	24.7	24.8
Cycle burnup accumulation (GWd/MTU)	21.5 / 18.3 / 8.0	31.7 / 25.6 / 12.1	32.6 / 27.7/ 12.3
Cycle-average specific power (MW/MTU)	29.4 / 25.1 / 11.0	43.4 / 35.0 / 16.6	44.6 / 37.9 / 16.8

Baseline fuel parameters such as enrichment, burnup, and power history for both LEU PWR and BWR fuel were first identified. These same parameters were then identified for LEU+ fuel. Next, source terms were generated and decay calculations were performed for all fuel types for use in thermal and shielding analysis.

Using the decay heat of each assembly type, thermal analysis of dry storage casks is performed and the PCT of the baseline cases are compared with the LEU+ cases. The additional cooling time required for the LEU+ cases to match the thermal performance of the corresponding baseline case is calculated. The highest-contributing nuclides to decay heat are calculated and compared across baseline and LEU+ cases. For PWR fuel, the decay heat and PCT sensitivity to the amount and configuration of burnable absorbers (IFBA and wet annular burnable absorber [WABA]) was also investigated. Additional cooling times required for LEU+ fuel to be loaded into representative regionalized dry storage loading patterns are calculated.

The calculated source terms were used to perform shielding calculations of dry storage casks, and the dose rates of the baseline cases were compared with the LEU+ cases. The additional cooling time required for the LEU+ cases to match the shielding performance of the corresponding baseline case was calculated. For PWR fuel, the dose rate sensitivity to the amount and configuration of absorber material was also investigated.

3.1 FUEL PARAMETERS AND SOURCE TERM GENERATION

3.1.1 Baseline Assembly Parameters

Spent fuel studies typically rely on assembly-level calculations with a few simplifications, such as constant power history without downtime between cycles and rounded irradiation times/specific powers, to produce a desired burnup. Assumed assembly irradiation parameters for the baseline cases are provided in Table 7 based on the LEU baseline data from Table 5 and Table 6. PWR studies assume a 17 × 17 assembly (Westinghouse design), and BWR studies assume a 10 × 10 bundle (GE14 design). The baseline cooling times are reasonable for current LEU fuel but may result in dose rates and PCTs that are higher than those in typical spent fuel storage system applications. For this analysis, these cooling times were

mainly selected to establish baselines against which to compare fuel with extended burnup and enrichment.

Table 7. Baseline assembly parameters.

Parameter	17 × 17 PWR	10 × 10 BWR
Average enrichment (wt %)	5.0	4.3
Uranium mass (kg)	522[1]	179[2]
Irradiation time (days)	1,500	2,200
Specific power (MW/MTU)	36.8	25
Discharge burnup (GWd/MTU)	55	55
Post-discharge cooling time (years)	6	6

1 Conservative assumption all mass is U.
2 Conservative assumption all fuel rods are full length.

3.1.2 Extended Enrichment Fuel Parameters

Two extended fuel enrichments were analyzed for both PWR and BWR fuel. These LEU+ assembly parameters are provided in Table 8. These fuel parameters were adapted from expected fuel behavior analyzed in Bae, Mertyurek, and Asgari [10] and represent reasonable values of burnup for LEU+ fuel. The power histories of the fuel were assumed to be constant with no downtime.

Table 8. LEU+ assembly parameters.

Parameter	17 × 17 PWR (6.5 wt %)	17 × 17 PWR (8.0 wt %)	10 × 10 BWR (6.6 wt %)	10 × 10 BWR (7.9 wt %)
Average enrichment (wt %)	6.5	8.0	6.6	7.9
Uranium mass (kg)	522	522	179	179
Irradiation time (days)	2,100	2,800	2,880	3,200
Specific power (MW/MTU)	34.3	28.6	25	25
Discharge burnup (GWd/MTU)	72	80	72	80
Post-discharge cooling time (years)	6	6	6	6

3.1.3 PWR Absorber Configurations

For the 17 × 17 PWR fuel assembly, various amounts and configurations of IFBA and WABA burnable absorber are analyzed. Gadolinium may be used in PWRs for additional reactivity hold-down, and optimized LEU+ assemblies with Gd were developed in the associated lattice work [10] but were not used in LEU+ core studies [8], [9]; thus, representative operating histories were unavailable at the time of this work. The amount of absorber rods in each configuration analyzed is provided in Table 9. The absorber configurations are shown in Figure 5 and Figure 6. In these figures, the fuel rods without IFBA are red, the fuel rods with IFBA are orange, and WABA is the annular material in the guide tubes only in Figure 6.

Table 9. Number of burnable absorbers.

Fuel lattice	IFBA	WABA
Minimum absorber	80	-
Maximum absorber	200	24

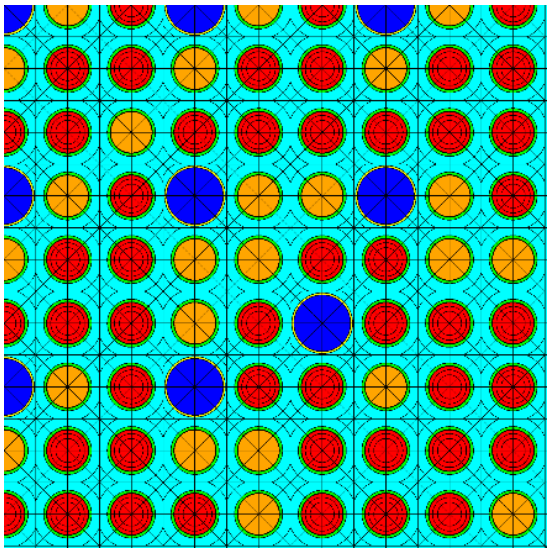

Figure 5. Southeast quarter of 17 × 17 assembly with 80 IFBA (red-colored) rods and 184 UO_2 (yellow-colored) rods.

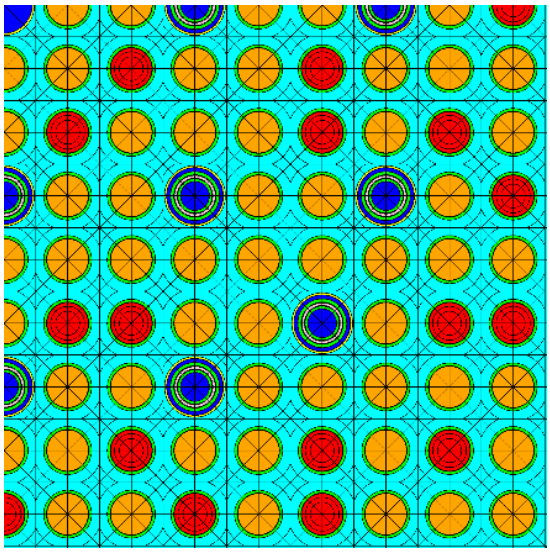

Figure 6. Southeast quarter of 17 × 17 assembly with 200 IFBA (red-colored) rods, 64 UO_2 (yellow-colored) rods, and 24 WABA (blue-colored) rods.

3.1.4 BWR Pin Maps

For the 10 × 10 BWR fuel assembly, various lattice-average enrichments were analyzed. These configurations represent the range of possible lattice-average enrichments [10]. The 10 × 10 BWR fuel assembly is shown in Figure 7. Pin maps and Gd concentrations are provided for each lattice-average enrichment analyzed in Figure 8 (baseline 4.3 wt %), Figure 9 (6.6 wt %), and Figure 10 (7.9 wt %). In each figure, the pin-wise distribution of fuel enrichment is shown on the left side of the figure, and the pin-wise distribution of Gd weight percent is shown on the right side. The amount of Gd increases for higher lattice-average enrichments.

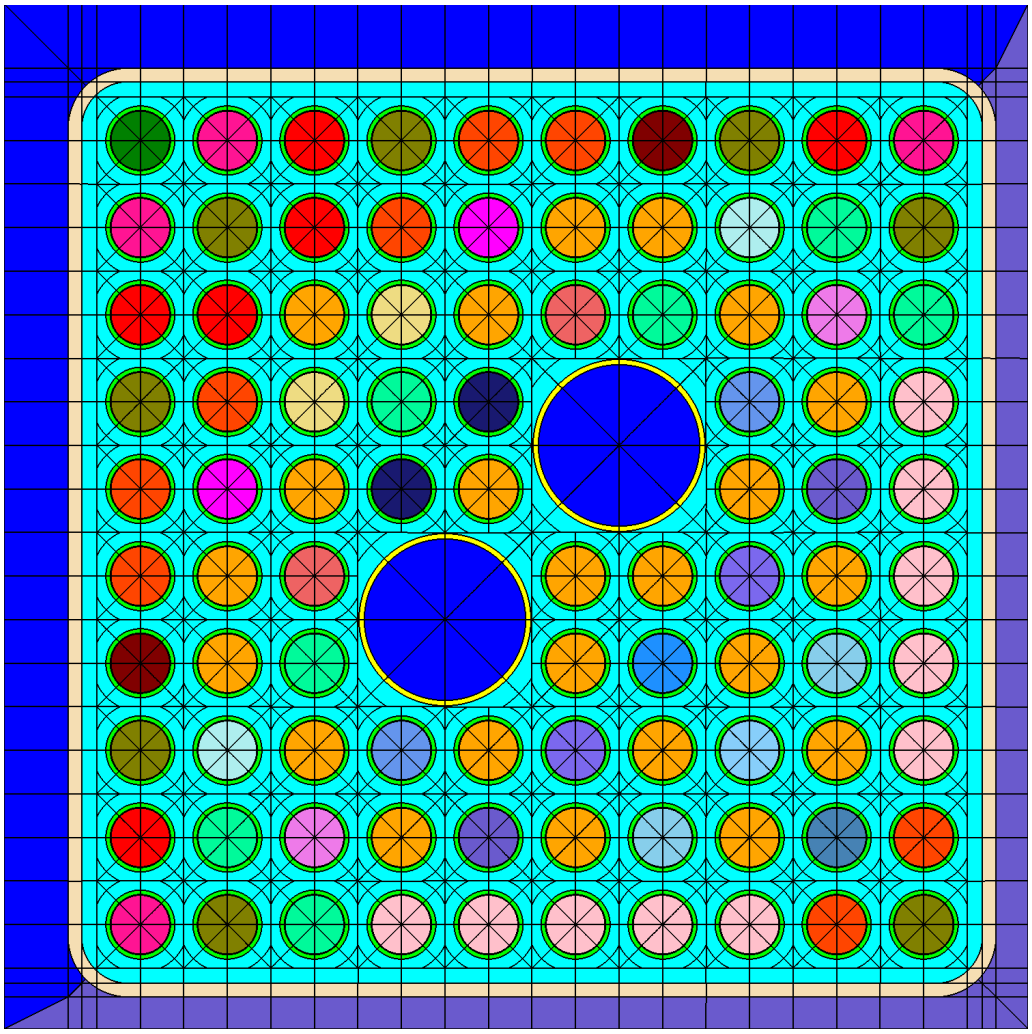

Figure 7. 10 × 10 BWR fuel assembly.

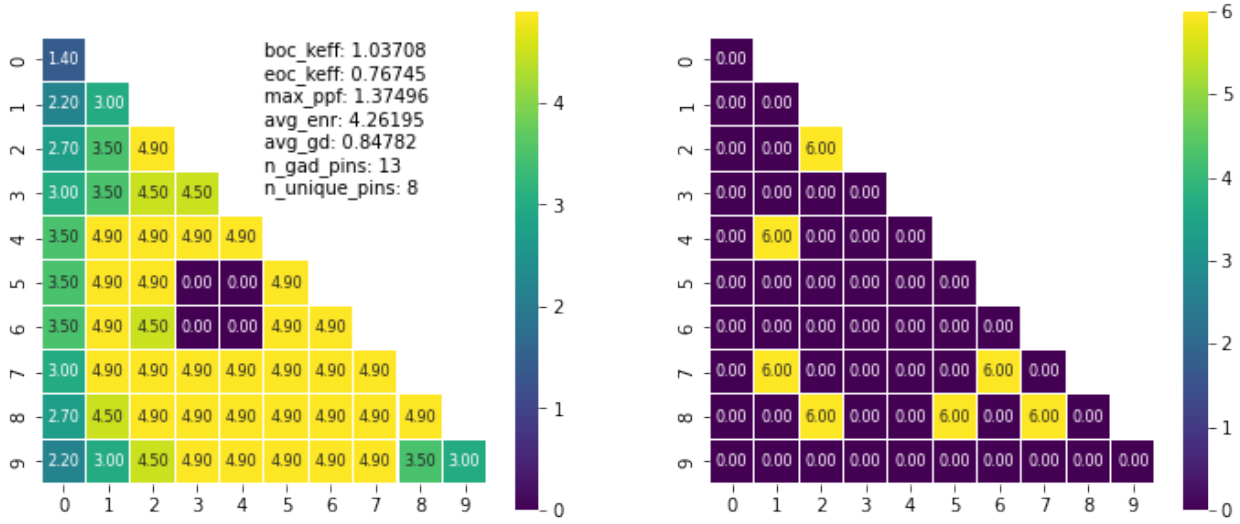

Figure 8. UO_2 enrichment pin map (left) and gadolinia rod distribution and Gd weight percent (right) for 4.3 wt % 10 × 10 BWR fuel assembly.

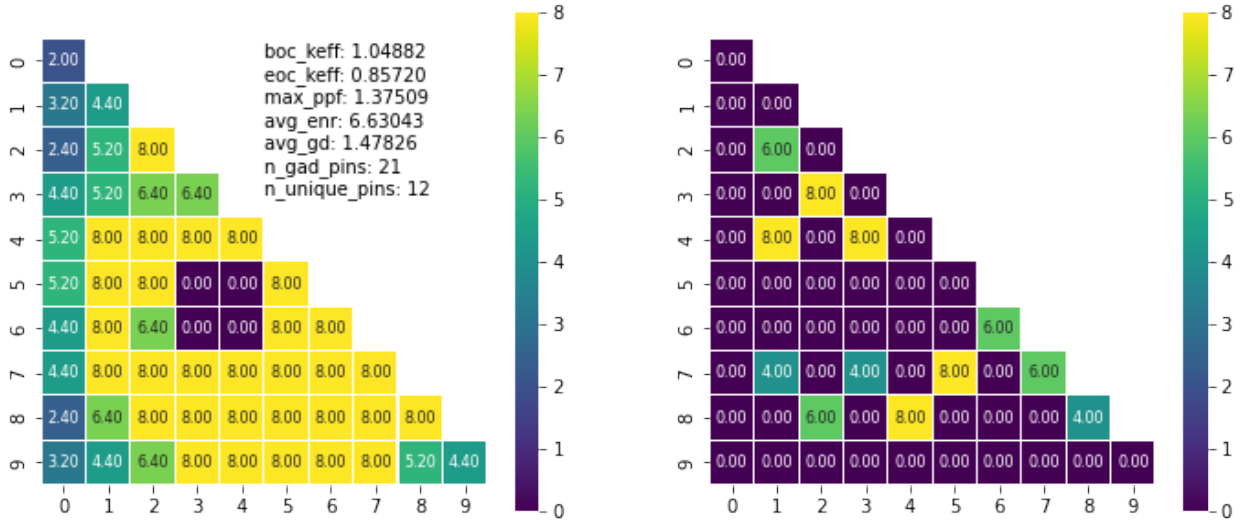

Figure 9. Enrichment pin map (left) and gadolinia rod distribution and Gd weight percent (right) for 6.6 wt % 10 × 10 BWR fuel assembly.

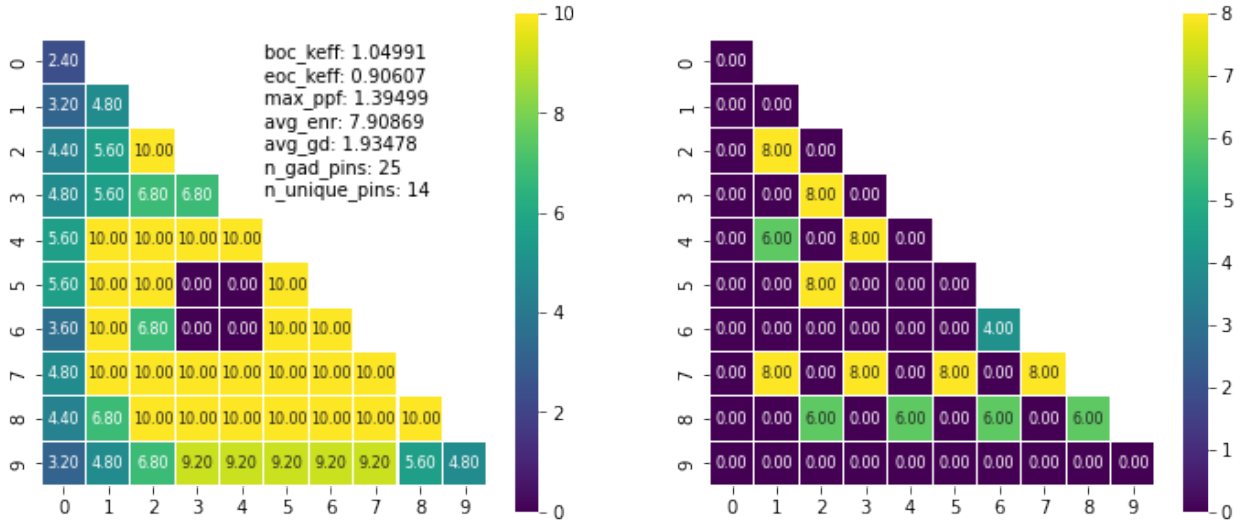

Figure 10. Enrichment pin map (left) and gadolinia rod distribution and Gd weight percent (right) for 7.9 wt % 10 × 10 BWR fuel assembly.

3.1.5 Source Term Generation

3.1.5.1 PWR Source Term Generation

SCALE/Polaris was used to perform a depletion calculation and generate ORIGEN cross-section libraries for each fuel assembly configuration. For each of the three PWR enrichments and two absorber configurations, a single cross-section library was generated up to a burnup of 80 GWd/MTU. Each assembly is quarter-symmetric, so only the southeast quarter was modeled. The power history is modeled as constant in Polaris, and no downtime was included. Each Polaris calculation was performed using a 56-group cross-section library. Material compositions, temperatures, and component dimensions used in the

Polaris models are provided in Table 10, Table 11, and Table 12, respectively. These parameters are adapted from Bae, Mertyurek, and Asgari [10] and are representative of PWR fuel.

Table 10. Polaris model material compositions.

Material densities	
Material	**Density (g/cm^3)**
Fuel	10.26
IFBA coating (ZrB_2)	3.85
WABA absorber	3.65
IFBA coating ^{10}B enrichment	
Isotope	**^{10}B enrichment (wt %)**
IFBA coating (ZrB_2)	50
Composition of WABA absorber	
Element/isotope	**Concentration (atoms/b-cm)**
^{10}B	2.98553E-3
^{11}B	1.21192E-2
Carbon	3.77001E-3
^{16}O	5.85563E-2
^{27}Al	3.90223E-2

Table 11. Polaris model material temperatures.

Material	**Temperature (K)**
Coolant	590
Moderator	590
Fuel	900
Cladding	700
Instrument tube	580
All other materials	590

Table 12. Polaris model fuel dimensions.

Component	**Dimension (cm)**
Pin pitch	1.260
Fuel pellet radius	0.4096
IFBA coating radius	0.4106
Gap radius	0.418
Cladding radius	0.475
Instrument tube inner radius	0.559
Instrument tube outer radius	0.605
Guide tube inner radius	0.561
Guide tube outer radius	0.602
WABA inner clad inner radius	0.286
WABA inner clad outer radius	0.339
WABA poison inner radius	0.353
WABA poison outer radius	0.404
WABA cladding inner radius	0.418
WABA cladding outer radius	0.484

3.1.5.2 BWR Source Term Generation

SCALE/Polaris was used to perform a depletion calculation and produce ORIGEN cross-section libraries for each BWR fuel lattice. Each assembly is half-symmetric, so only one half of the assembly was

modeled. Partial-length fuel rods and enrichment blankets were not considered in this analysis. The power history was modeled as constant in Polaris, and no downtime was included. Each Polaris calculation was performed using a 56-group cross-section library. Material compositions, temperatures, and component dimensions used in the Polaris models adapted from Bae, Mertyurek, and Asgari [10] are provided in Table 13, Table 14, and Table 15, respectively. The two-phase coolant density corresponds to 40% void, and the single-phase coolant, which is defined as water outside of the channel box with no direct heating, corresponds to saturation conditions at system pressure or 0% void.

Table 13. BWR Polaris model material compositions.

Material	Density (g/cm^3)
Fuel	10.64
Fuel + Gd_2O_3	10.4462
Two-phase coolant	0.42147
Single-phase coolant	0.73511

Table 14. BWR Polaris model material temperatures.

Material	Temperature (K)
Fuel	792.4
Cladding	700.0
Instrument tube	561.4
All other materials	561.4

Table 15. BWR Polaris model fuel dimensions.

Component	Dimension (cm)
Pin pitch	1.2954
Fuel pellet radius	0.438
Gap radius	0.447
Cladding radius	0.513
Water rod tube inner radius	1.200
Water rod tube outer radius	1.280
Half-distance between assemblies (east and south)	0.47498
Half-distance between assemblies (north and west)	0.9525
Box thickness	0.2032
Inner corner radius	0.700
Half inner span	6.70306

3.2 PWR DRY STORAGE CASK ANALYSIS

3.2.1 Decay Heat and PCT Calculations

Decay heats and PCT values were calculated using COBRA-SFS for storage casks that contained PWR fuel with parameters that covered the range of enrichments, cooling times, and absorber configurations. The primary input to the COBRA-SFS PCT calculations was the decay heat of each assembly loaded into the cask. A depletion/decay calculation was performed for each fuel type by using SCALE/ORIGAMI. The decay heat of each fuel type at the same cooling time is provided in Table 16.

Table 16. Decay heat of PWR fuel types.

Fuel	Burnup (GWd/MTU)	Cooling time (years)	Decay heat (kW)
Baseline (5.0 wt %)	55	6	1.50
LEU+ (6.5 wt %)	72	6	2.05
LEU+ (8.0 wt %)	80	6	2.20

3.2.1.1 Baseline Case

PCT for the baseline case was calculated for the General-37 storage cask type in UNF-ST&DARDS. All PCT calculations were performed assuming that fuel with one enrichment, burnup, cooling time, and absorber configuration is uniformly loaded into every cell of the cask. The calculated PCT for the baseline case was 944°F. Although the calculated baseline PCT exceeds the limit of 752°F, which is suggested in ISG-11 [11] to meet cladding requirements for storage [12], a real cask would not be uniformly loaded with such relatively high-burned and low-cooled fuel in this manner. These results only serve to create a baseline against which to compare decay heat and PCT for casks loaded with LEU+ PWR fuel.

3.2.1.2 LEU+ Cases

The decay heats and PCT for the LEU+ PWR cases were calculated for the General-37 storage cask type in UNF-ST&DARDS. All PCT calculations were performed assuming that one fuel type and absorber configuration is uniformly loaded into every cell of the cask. PCT results for the LEU+ PWR cases are provided in Table 17. The PCT increased with increasing burnup and enrichment.

Table 17. LEU+ PWR canister decay heat and PCT results.

Enrichment (wt %)	Burnup (GWd/MTU)	Cooling time (years)	Canister decay heat (kW)	PCT (°F)
5.0	55	6.0	55.5	944.0
6.5	72	6.0	75.9	1186.6
8.0	80	6.0	81.4	1249.8

For each LEU+ PWR assembly, the additional cooling time required to match the baseline PCT value was also calculated. The additional cooling time was calculated by repeating the PCT calculation at several cooling times, plotting PCT as a function of cooling time, fitting a power function to the data, and then using the function to calculate the cooling time required to match the baseline PCT value. The plots of PCT vs. cooling time for the 6.5 wt % fuel and the 8 wt % fuel are provided in Figure 11 and Figure 12, respectively. The fit was then used to determine the amount of additional cooling time that the canister would require to return to the original PCT value. The additional cooling times required for each LEU+ PWR fuel to match the baseline PCT value are provided in Table 18. The results in Table 18 indicate that it would require between 5.82 and 8.87 additional years to return to the original PCT values for the LEU+/HBU scenarios.

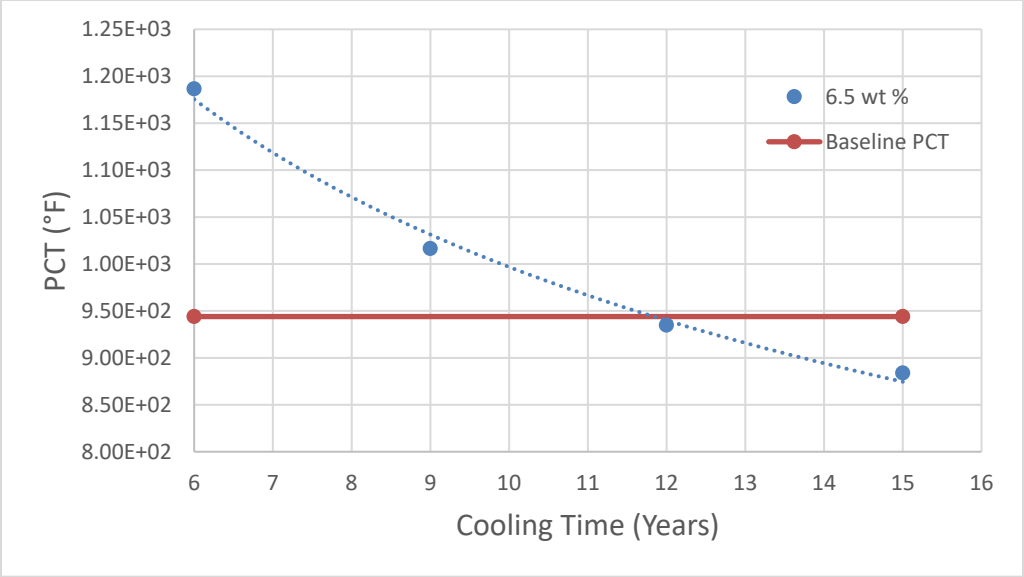

Figure 11. PCT vs. cooling time for General-37 loaded with 6.5 wt % LEU+ PWR fuel.

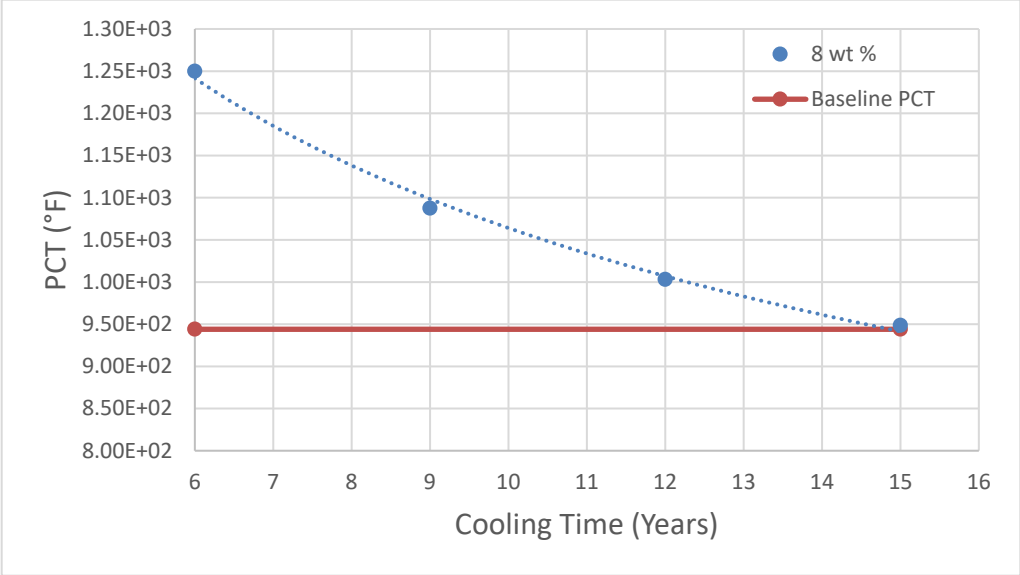

Figure 12. PCT vs. cooling time for General-37 loaded with 8 wt % LEU+ PWR fuel.

Table 18. Additional cooling time required for LEU+ PWR fuel to match baseline PCT.

LEU+ fuel	Cooling time (years)	Additional cooling time (years)
6.5 wt %	11.8	5.82
8.0 wt %	14.9	8.87

3.2.1.3 Decay Heat and PCT Sensitivity to Absorbers

The analyses discussed in Section 3.2.1.2 studied the effects of LEU+/HBU configurations without considering the need for increased absorber loadings. Increased enrichments necessitate increased burnable absorber loadings to support in-core fuel management requirements. The effect of the amount and configuration of absorbing material on the decay heat of the W 17 × 17 STD PWR fuel assembly was analyzed. The baseline case, which is loaded with 80 IFBA rods, was compared with the maximum absorber configuration, which is loaded with 200 IFBA rods and 24 WABA rodlets. Additional Polaris calculations were performed to develop ORIGEN libraries with the maximum absorber configuration for the 5.0, 6.5, and 8.0 wt % enrichment cases. For each enrichment, the maximum absorber configuration was compared with the 80 IFBA used in the baseline configuration. Assuming that fuel with each absorber configuration was uniformly loaded into the General-37 cask, the PCT was also calculated. Decay heat calculations were performed by using ORIGAMI at a fixed cooling time of 6 years for each fuel enrichment and absorber configuration. PCTs were then calculated using these decay heat values. Calculated values of decay heat and PCT for each PWR fuel enrichment and absorber configuration are provided in Table 19. These results demonstrate that the amount and configuration of absorbing material in the analyzed PWR lattices did not significantly affect the decay heat of the assembly or the PCT once loaded into the cask at the relatively low cooling time analyzed.

Table 19. Decay heat of each PWR fuel enrichment and absorber configuration.

5.0 wt % (baseline)		
Absorber configuration	**Assembly decay heat (kW)**	**PCT (°F)**
Baseline	1.50	944.0
Maximum	1.49	939.4
6.5 wt %		
Absorber configuration	**Assembly decay heat (kW)**	**PCT (°F)**
Baseline	2.05	1,186.6
Maximum	2.04	1,182.3
8.0 wt %		
Absorber configuration	**Assembly decay heat (kW)**	**PCT (°F)**
Baseline	2.20	1,249.8
Maximum	2.19	1,245.7

3.2.1.4 Nuclide Contribution to Decay Heat

The nuclides with the highest per-assembly decay heat contribution (generally on the order of 10 W or greater) were calculated as part of the ORIGAMI decay calculation. These nuclides and their decay heats are provided in Tables 20, 21, and 22 for all PWR enrichment, cooling time, and absorber configurations analyzed. Generally, the highest-contributing nuclides did not depend on the absorber amount and configuration. For a given enrichment, the highest-contributing nuclides were also generally the same over the range of cooling times analyzed, aside from short-lived nuclides, such as ^{134}Cs and ^{106}Rh. For the burnups analyzed, the highest-contributing nuclides were generally the same with changing enrichment.

Table 20. Nuclides with highest contribution to PWR assembly decay heat (5 wt %).

Enrichment (wt %)	5.0			5.0		
Burnup (GWd/MTU)	55			55		
Cooling time (years)	6			6		
Absorber configuration	Baseline			Maximum		
	Nuclide	**Decay heat (W)**	**Percentage of total (%)**	**Nuclide**	**Decay heat (W)**	**Percentage of total (%)**
	^{90}Y	2.95E+02	19.6	^{90}Y	2.77E+02	18.6
	^{137m}Ba	2.91E+02	19.4	^{137m}Ba	2.76E+02	18.5
	^{134}Cs	2.33E+02	15.5	^{134}Cs	2.37E+02	15.9
	^{244}Cm	1.58E+02	10.5	^{244}Cm	1.62E+02	10.9
	^{238}Pu	1.49E+02	9.9	^{238}Pu	1.57E+02	10.5
	^{137}Cs	8.35E+01	5.5	^{137}Cs	8.34E+01	5.6
	^{106}Rh	6.40E+01	4.3	^{90}Sr	6.13E+01	4.1
	^{90}Sr	6.19E+01	4.1	^{106}Rh	6.12E+01	4.1
	Eu^{154}	4.08E+01	2.7	Eu^{154}	4.30E+01	2.9
	Am^{241}	3.94E+01	2.6	Am^{241}	4.24E+01	2.8
	^{144}Pr	2.45E+01	1.6	^{144}Pr	2.32E+01	1.6
	^{60}Co	1.55E+01	1.0	^{60}Co	1.56E+01	1.0

Table 21. Nuclides with highest contribution to PWR assembly decay heat (6.5 wt %).

Enrichment (wt %)	6.5			6.5			6.5			6.5			6.5		
Burnup (GWd/MTU)	72			72			72			72			72		
Cooling time (years)	6			9			12			15			6		
Absorber configuration	Minimum			Minimum			Minimum			Minimum			Maximum		
	Nuclide	Decay heat (W)	Percentage of total (%)	Nuclide	Decay heat (W)	Percentage of total (%)	Nuclide	Decay heat (W)	Percentage of total (%)	Nuclide	Decay heat (W)	Percentage of total (%)	Nuclide	Decay heat (W)	Percentage of total (%)
	^{90}Y	3.82E+02	18.6	^{90}Y	3.55E+02	21.4	^{90}Y	3.30E+02	22.3	^{90}Y	3.07E+02	22.5	^{90}Y	3.61E+02	17.7
	^{137m}Ba	3.74E+02	18.2	^{137m}Ba	3.49E+02	21.0	^{137m}Ba	3.26E+02	22.0	^{137m}Ba	3.04E+02	22.3	^{137m}Ba	3.56E+02	17.5
	^{134}Cs	3.15E+02	15.3	^{244}Cm	2.49E+02	15.0	^{238}Pu	2.42E+02	16.3	^{238}Pu	2.36E+02	17.3	^{134}Cs	3.19E+02	15.6
	^{244}Cm	2.79E+02	13.6	^{238}Pu	2.48E+02	14.9	^{244}Cm	2.22E+02	15.0	^{244}Cm	1.98E+02	14.5	^{244}Cm	2.83E+02	13.9
	^{238}Pu	2.54E+02	12.3	^{134}Cs	1.15E+02	6.9	^{137}Cs	9.33E+01	6.3	^{241}Am	8.92E+01	6.5	^{238}Pu	2.65E+02	13.0
	^{137}Cs	1.07E+02	5.2	^{137}Cs	9.99E+01	6.0	^{241}Am	7.74E+01	5.2	^{137}Cs	8.70E+01	6.4	^{137}Cs	1.07E+02	5.3
	^{90}Sr	8.01E+01	3.9	^{90}Sr	7.45E+01	4.5	^{90}Sr	6.93E+01	4.7	^{90}Sr	6.45E+01	4.7	^{90}Sr	7.94E+01	3.9
	^{106}Rh	6.51E+01	3.2	^{241}Am	6.36E+01	3.8	^{134}Cs	4.20E+01	2.8	^{154}Eu	2.72E+01	2.0	^{106}Rh	6.25E+01	3.1
	^{154}Eu	5.62E+01	2.7	^{154}Eu	4.42E+01	2.7	^{154}Eu	3.47E+01	2.3	^{134}Cs	1.53E+01	1.1	^{154}Eu	5.90E+01	2.9
	^{241}Am	4.75E+01	2.3	^{60}Co	1.12E+01	0.7	^{240}Pu	1.00E+01	0.7	^{240}Pu	1.01E+01	0.7	^{241}Am	5.10E+01	2.5
	^{144}Pr	2.30E+01	1.1	^{240}Pu	9.96E+00	0.6	^{239}Pu	8.10E+00	0.5	^{239}Pu	8.10E+00	0.6	^{144}Pr	2.19E+01	1.1
	^{60}Co	1.66E+01	0.8	^{106}Rh	8.43E+00	0.5	^{60}Co	7.55E+00	0.5	^{85}Kr	5.55E+00	0.4	^{60}Co	1.67E+01	0.8
	^{85}Kr	9.91E+00	0.5	^{85}Kr	8.17E+00	0.5	^{85}Kr	6.73E+00	0.5	^{60}Co	5.09E+00	0.4	^{240}Pu	1.03E+01	0.5

Table 22. Nuclides with highest contribution to PWR assembly decay heat (8 wt %).

Enrichment (wt %)	8			8			8			8			8		
Burnup (GWd/MTU)	80			80			80			80			80		
Cooling time (years)	6			9			12			15			6		
Absorber configuration	Minimum			Minimum			Minimum			Minimum			Maximum		
	Nuclide	Decay heat (W)	Percentage of total (%)	Nuclide	Decay heat (W)	Percentage of total (%)	Nuclide	Decay heat (W)	Percentage of total (%)	Nuclide	Decay heat (W)	Percentage of total (%)	Nuclide	Decay heat (W)	Percentage of total (%)
	^{90}Y	4.29E+02	19.5	^{90}Y	3.99E+02	22.0	^{90}Y	3.72E+02	22.8	^{90}Y	3.46E+02	22.9	^{90}Y	4.08E+02	18.6
	^{137m}Ba	4.07E+02	18.4	^{137m}Ba	3.79E+02	20.9	^{137m}Ba	3.54E+02	21.7	^{137m}Ba	3.30E+02	21.9	^{137m}Ba	3.89E+02	17.7
	^{134}Cs	3.14E+02	14.2	^{238}Pu	3.03E+02	16.7	^{238}Pu	2.96E+02	18.1	^{238}Pu	2.89E+02	19.2	^{238}Pu	3.24E+02	14.8
	^{238}Pu	3.10E+02	14.1	^{244}Cm	2.47E+02	13.6	^{244}Cm	2.20E+02	13.5	^{244}Cm	1.96E+02	13.0	^{134}Cs	3.18E+02	14.5
	^{244}Cm	2.77E+02	12.5	^{134}Cs	1.15E+02	6.3	^{137}Cs	1.01E+02	6.2	^{241}Am	9.75E+01	6.5	^{244}Cm	2.81E+02	12.8
	^{137}Cs	1.16E+02	5.3	^{137}Cs	1.09E+02	6.0	^{241}Am	8.49E+01	5.2	^{137}Cs	9.47E+01	6.3	^{137}Cs	1.16E+02	5.3
	^{90}Sr	9.01E+01	4.1	^{90}Sr	8.38E+01	4.6	^{90}Sr	7.80E+01	4.8	^{90}Sr	7.25E+01	4.8	^{90}Sr	8.94E+01	4.1
	^{154}Eu	6.33E+01	2.9	^{241}Am	7.02E+01	3.9	^{134}Cs	4.19E+01	2.6	^{154}Eu	3.07E+01	2.0	^{154}Eu	6.63E+01	3.0
	^{106}Rh	5.36E+01	2.4	^{154}Eu	4.97E+01	2.7	^{154}Eu	3.91E+01	2.4	^{134}Cs	1.53E+01	1.0	^{241}Am	5.67E+01	2.6
	^{241}Am	5.30E+01	2.4	^{60}Co	1.01E+01	0.6	^{240}Pu	1.01E+01	0.6	^{240}Pu	1.02E+01	0.7	^{106}Rh	5.18E+01	2.4
	^{144}Pr	1.94E+01	0.9	^{240}Pu	1.00E+01	0.6	^{239}Pu	8.87E+00	0.5	^{239}Pu	8.87E+00	0.6	^{144}Pr	1.86E+01	0.8
	^{60}Co	1.50E+01	0.7	^{239}Pu	8.87E+00	0.5	^{85}Kr	7.26E+00	0.4	^{85}Kr	5.99E+00	0.4	^{60}Co	1.52E+01	0.7
	^{85}Kr	1.07E+01	0.5	^{85}Kr	8.81E+00	0.5	^{60}Co	6.82E+00	0.4	^{60}Co	4.60E+00	0.3	^{85}Kr	1.06E+01	0.5
	^{240}Pu	9.97E+00	0.5	^{106}Rh	6.95E+00	0.4	^{241}Pu	2.77E+00	0.2	^{241}Pu	2.39E+00	0.2	^{240}Pu	1.03E+01	0.5

3.2.1.5 Cooling Time Requirements for Regionalized Loading

Dry storage casks are typically licensed to load fuel using regionalized loading patterns. These regionalized patterns enforce regional- or cell-wise decay heat limits. Regionalized loading patterns allow for high-decay heat, typically high-burned or low-cooled, assemblies to be loaded because their effect on the cask-total decay heat and dose rates is offset by also loading low-decay heat (low-burned or long-cooled) assemblies. For each of the PWR enrichments analyzed, the cooling time required to produce a decay heat representative of a typical dry storage cask cell limit using regionalized loading was calculated. ORIGAMI decay calculations were performed over a wide range of cooling times. An exponential function was fit to the data, and cooling time requirements for each decay heat were calculated. The cooling times required to meet the representative decay heat limits are provided in Table 23. The calculated cooling times indicate that LEU+ fuel likely must be stored in basket cells with high decay heat limits to store these assemblies with a reasonable amount of cooling time.

Table 23. PWR cooling time requirements for regionalized loading representative decay heat values.

Enrichment (wt %)	**5**	**6.5**	**8**
Burnup (GWd/MTU)	**55**	**72**	**80**
Decay heat (W)	**Cooling time (years)**	**Cooling time (years)**	**Cooling time (years)**
300	90	125	138
500	60	88	99
700	40	64	73
1,000	19	39	46
1,500	7	10	14

3.2.2 Shielding Calculations

Dose rates were calculated using SCALE/MAVRIC for storage casks that contained PWR fuel with parameters covering a range of enrichments, cooling times, and absorber configurations.

3.2.2.1 Shielding Baseline Case

Dose rates for the baseline cases were calculated for the General-37 storage cask type in UNF-ST&DARDS. Dose rate calculations were performed assuming that one fuel type and absorber configuration were uniformly loaded into every cell of the cask. The maximum dose rate at the mid-height on the external surface of the cask for the baseline case is provided in Table 24. For this analysis, the dose rate at the mid-height on the external surface of the cask was selected as a representative dose point against which to compare dose rates for LEU+ fuel. The baseline does rates may be higher than expected because of the uniform loading with relatively high-burned fuel cooled for a short time. However, these results only serve to create a baseline against which to compare dose rates for casks loaded with LEU+ fuel.

3.2.2.2 Shielding Extended Enrichment Cases

Dose rates for the LEU+ cases were calculated for the General-37 storage cask type in UNF-ST&DARDS. Dose rate calculations were performed assuming that one fuel type and absorber configuration were uniformly loaded into every cell of the cask. The maximum dose rates at the mid-height on the external cask surface for the LEU+ cases are provided in Table 24. Neutron dose rates are generally expected to decrease with increased enrichment at constant burnup [13]. However, the external dose rate of a concrete storage cask is dominated by gamma dose rate because the concrete overpack

significantly attenuates the neutron source due to its hydrogen content. The gamma dose rate is directly proportional to fuel burnup and it is not significantly sensitive to fuel enrichment [13].

Table 24. LEU+ PWR dose rate results.

Enrichment	Burnup (GWd/MTU)	Cooling time (years)	Dose rate (mrem/h)	Relative uncertainty (%)
5.0	55	6.0	7.04E+01	2.9
6.5	72	6.0	8.94E+01	2.49
8.0	80	6.0	9.39E+01	4.34

For each LEU+ assembly, the additional cooling time required to approximately match the baseline dose rate was also calculated. The additional cooling time was calculated by repeating the dose rate calculation at several cooling times, plotting the dose rate as a function of cooling time, fitting a power function to the data, and then using the function to calculate the cooling time required to match the baseline dose rate value. The plots of maximum mid-height surface dose rate vs. cooling time for the 6.5 wt % fuel and the 8 wt % fuel are provided in Figure 13 and Figure 14, respectively. The additional cooling times required for each LEU+ fuel to match the baseline dose rate value are provided in Table 25 and show that the increases in required cooling time to match the baseline dose rate is approximately 1.5 years. However, the required additional cooling time may vary depending on the type of overpack (i.e., transportation or storage) and baseline cooling time.

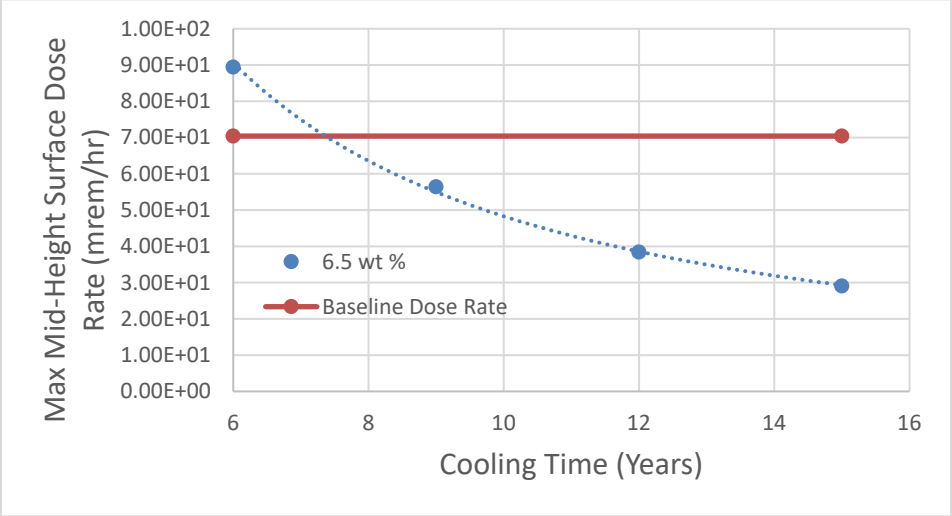

Figure 13. Maximum mid-height surface dose rate vs. cooling time for General-37 loaded with 6.5 wt % PWR fuel.

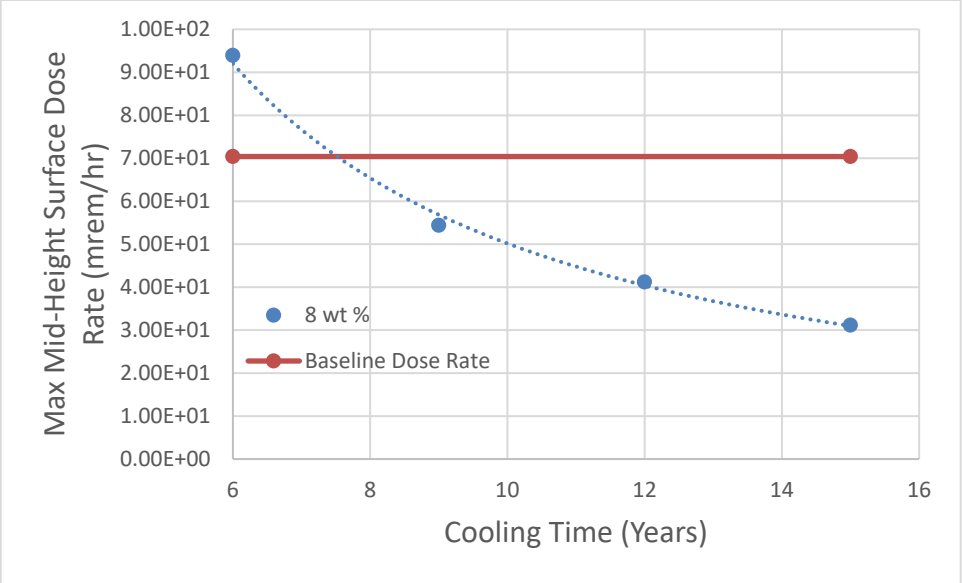

Figure 14. Maximum mid-height surface dose rate vs. cooling time for General-37 loaded with 8 wt % PWR fuel.

Table 25. Additional cooling time required for LEU+ PWR fuel to match baseline maximum mid-height surface dose rate.

LEU+ fuel	Cooling time (years)	Additional cooling time (years)
6.5 wt %	7.37	1.37
8.0 wt %	7.51	1.51

3.2.2.3 Dose Rate Sensitivity to Absorbers

The effect of the amount and configuration of absorbing material on the dose rates external to a cask loaded with W 17 × 17 STD PWR fuel was analyzed. Fuel with a specified absorber configuration was assumed to be uniformly loaded into the General-37 cask. Calculated maximum mid-height surface dose rates for each PWR fuel enrichment and absorber configuration are provided in Table 26. These results demonstrate that the amount and configuration of absorbing material in the analyzed PWR lattices do not considerably affect the maximum mid-height surface dose rate of a storage cask at the relatively low cooling time analyzed.

Table 26. Maximum mid-height surface dose rate of General-37 loaded with each PWR fuel enrichment and absorber configuration.

5.0 wt % (baseline)		
Absorber configuration	**Dose rate (mrem/h)**	**Relative uncertainty (%)**
Minimum	7.04E+01	2.29
Maximum	7.45E+01	14.74
6.5 wt %		
Absorber configuration	**Dose rate (mrem/h)**	**Relative uncertainty (%)**
Minimum	8.94E+01	2.49
Maximum	9.05E+01	2.55
8.0 wt %		
Absorber configuration	**Dose rate (mrem/h)**	**Relative uncertainty (%)**
Minimum	9.39E+01	4.34
Maximum	9.26E+01	2.38

3.3 BWR DRY STORAGE CASK ANALYSIS

3.3.1 Decay Heat and PCT Calculations

Decay heats and PCT were calculated by using COBRA-SFS for storage casks that contained BWR fuel with parameters that covered the range of lattice-average enrichments and cooling times.

The primary input to the COBRA-SFS PCT calculations was the decay heat of each assembly loaded into the cask. A depletion/decay calculation was performed for each fuel type by using SCALE/ORIGAMI. The decay heat of each fuel type at the same cooling time is provided in Table 27.

Table 27. Decay heat of BWR fuel types.

Fuel	Burnup (GWd/MTU)	Cooling time (years)	Decay heat (kW)
Baseline (4.3 wt %)	55	6	0.50
LEU+ (6.6 wt %)	72	6	0.67
LEU+ (7.9 wt %)	80	6	0.74

3.3.1.1 Baseline Case

Because of the availability of existing analysis models, PCT for the BWR baseline case was calculated for the General-68 storage cask type in UNF-ST&DARDS. All PCT calculations were performed assuming that fuel with one lattice-average enrichment, burnup, and cooling time is uniformly loaded into every cell of the cask. The calculated PCT for the BWR baseline case was 493.6 °F. A real cask would not be uniformly loaded with such relatively high-burned and low-cooled fuel in this manner; these results only serve to create a baseline against which to compare decay heat and PCT for casks loaded with LEU+ BWR fuel.

3.3.1.2 Extended Enrichment Cases

PCT for the extended enrichment BWR cases were calculated for the General-68 storage cask type in UNF-ST&DARDS. All PCT calculations were performed assuming that fuel with one lattice-average enrichment, burnup, and cooling time is uniformly loaded into every cell of the cask. PCT results for the LEU+ BWR cases are provided in Table 28. The PCT increased with increasing burnup and lattice-average enrichment.

Table 28. LEU+ BWR PCT results.

Enrichment (wt %)	Burnup (GWd/MTU)	Cooling time (years)	Canister decay heat (kW)	PCT (°F)
4.3	55	6.0	34.0	493.6
6.6	72	6.0	45.6	616.3
7.9	80	6.0	50.3	631.3

For each LEU+ BWR assembly, the additional cooling time required to match the baseline PCT value was also calculated. The additional cooling time was calculated by repeating the PCT calculation at several cooling times, plotting PCT as a function of cooling time, fitting a power function to the data, and then using the function to calculate the cooling time required to match the baseline PCT value. The plots of PCT versus cooling time for the 6.6 wt % fuel and the 7.9 wt % BWR fuel are provided in Figure 15 and Figure 16, respectively. The additional cooling times required for each LEU+ BWR fuel to match the baseline PCT value are provided in Table 29.

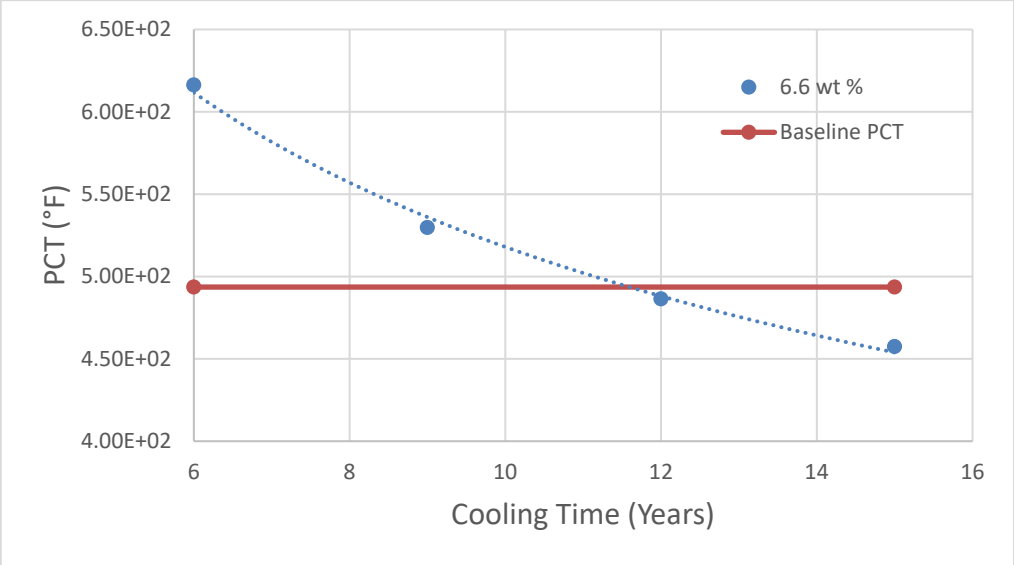

Figure 15. PCT vs. cooling time for General-68 loaded with 6.6 wt % LEU+ BWR fuel.

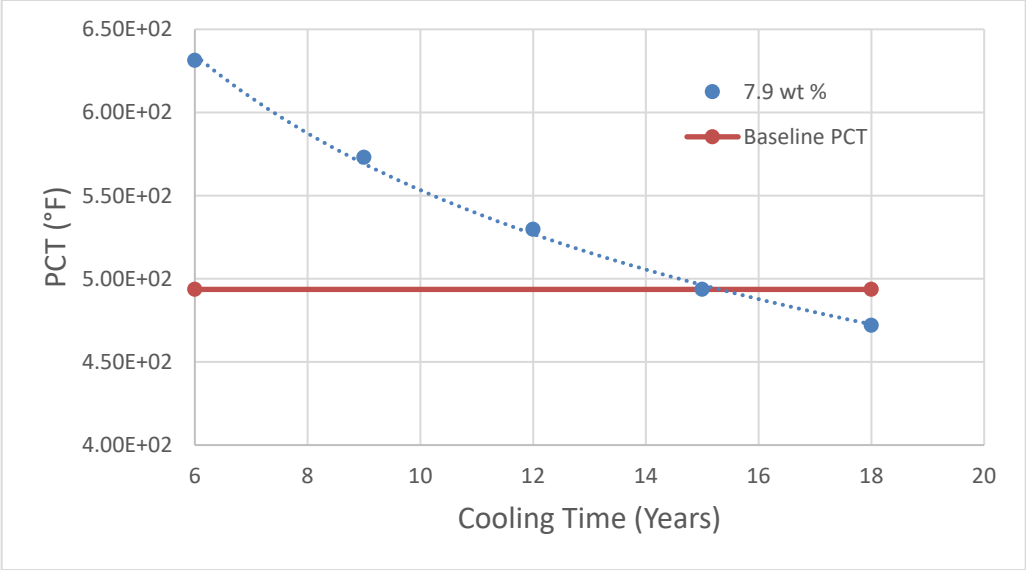

Figure 16. PCT vs. cooling time for General-68 loaded with 7.9 wt % LEU+ BWR fuel.

Table 29. Additional cooling time required for LEU+ BWR fuel to match baseline PCT.

Lattice-average enrichment (wt %)	Cooling time (years)	Additional cooling time (years)
6.6	11.6	5.56
7.9	15.4	9.36

3.3.1.3 Nuclide Contribution to Decay Heat

The nuclides with the highest per-assembly decay heat contribution (generally on the order of 10 W or greater) were calculated as part of the ORIGAMI decay calculation. These nuclides and their decay heats are provided in Table 30, Table 31, and Table 32 for all BWR lattices and cooling times analyzed. Generally, the highest-contributing nuclides were shown not to depend strongly on the lattice-average enrichment or the Gd concentration at the burnups analyzed in this work. At these burnups, the absorbing material was likely depleted; lesser-burned fuel may result in different highest-contributing nuclides. For a given lattice-average enrichment, the highest-contributing nuclides were also generally the same over the range of cooling times analyzed, aside from short-lived nuclides such as ^{134}Cs and ^{106}Rh.

Table 30. Nuclides with highest contribution to BWR assembly decay heat (4.3 wt %).

Lattice-average enrichment (wt %)	4.3		
Burnup (GWd/MTU)	55		
Cooling time (years)	6		
	Nuclide	**Decay heat (W)**	**Percentage of total (%)**
	^{137m}Ba	9.58E+01	19.0
	^{90}Y	9.09E+01	18.0
	^{244}Cm	8.93E+01	17.7
	^{134}Cs	7.10E+01	14.1
	^{238}Pu	4.75E+01	9.4
	^{137}Cs	2.74E+01	5.4
	^{90}Sr	1.91E+01	3.8
	^{106}Rh	1.80E+01	3.6
	^{154}Eu	1.11E+01	2.2
	^{241}Am	9.33E+00	1.8
	^{60}Co	5.85E+00	1.2
	^{144}Pr	5.42E+00	1.1

Table 31. Nuclides with highest contribution to BWR assembly decay heat (6.6 wt %).

Lattice-average enrichment (wt %)	6.6											
Burnup (GWd/MTU)	72											
Cooling time (years)	6			9			12			15		
	Nuclide	Decay heat (W)	Percentage of total (%)	Nuclide	Decay heat (W)	Percentage of total (%)	Nuclide	Decay heat (W)	Percentage of total (%)	Nuclide	Decay heat (W)	Percentage of total (%)
	^{90}Y	1.23E+02	18.4	^{137m}Ba	1.14E+02	20.9	^{137m}Ba	1.07E+02	21.9	^{137m}Ba	9.96E+01	22.2
	^{137m}Ba	1.23E+02	18.4	^{90}Y	1.14E+02	20.9	^{90}Y	1.06E+02	21.8	^{90}Y	9.89E+01	22.0
	^{244}Cm	1.22E+02	18.3	^{244}Cm	1.09E+02	19.9	^{244}Cm	9.71E+01	19.9	^{244}Cm	8.66E+01	19.3
	^{134}Cs	9.05E+01	13.6	^{238}Pu	7.44E+01	13.6	^{238}Pu	7.26E+01	14.9	^{238}Pu	7.09E+01	15.8
	^{238}Pu	7.62E+01	11.4	^{134}Cs	3.31E+01	6.0	^{137}Cs	3.06E+01	6.3	^{137}Cs	2.85E+01	6.4
	^{137}Cs	3.51E+01	5.3	^{137}Cs	3.28E+01	6.0	^{90}Sr	2.23E+01	4.6	^{241}Am	2.10E+01	4.7
	^{90}Sr	2.58E+01	3.9	^{90}Sr	2.40E+01	4.4	^{241}Am	1.82E+01	3.7	^{90}Sr	2.07E+01	4.6
	^{106}Rh	1.73E+01	2.6	^{241}Am	1.50E+01	2.7	^{134}Cs	1.21E+01	2.5	^{154}Eu	7.22E+00	1.6
	^{154}Eu	1.49E+01	2.2	^{154}Eu	1.17E+01	2.1	^{154}Eu	9.20E+00	1.9	^{134}Cs	4.41E+00	1.0
	^{241}Am	1.13E+01	1.7	^{60}Co	3.85E+00	0.7	^{240}Pu	3.24E+00	0.7	^{240}Pu	3.26E+00	0.7
	^{60}Co	5.71E+00	0.9	^{240}Pu	3.21E+00	0.6	^{60}Co	2.60E+00	0.5	^{239}Pu	2.22E+00	0.5
	^{144}Pr	5.52E+00	0.8	^{85}Kr	2.48E+00	0.5	^{239}Pu	2.22E+00	0.5	^{60}Co	1.75E+00	0.4
	^{240}Pu	3.18E+00	0.5	^{106}Rh	2.24E+00	0.4	^{85}Kr	2.04E+00	0.4	^{85}Kr	1.68E+00	0.4

Table 32. Nuclides with highest contribution to BWR assembly decay heat (7.9 wt %).

Lattice-average enrichment (wt %)	7.9											
Burnup (GWd/MTU)	80											
Cooling time (years)	6			9			12			15		
	Nuclide	Decay heat (W)	Percentage of total (%)	Nuclide	Decay heat (W)	Percentage of total (%)	Nuclide	Decay heat (W)	Percentage of total (%)	Nuclide	Decay heat (W)	Percentage of total (%)
	^{90}Y	1.38E+02	18.8	^{90}Y	1.29E+02	21.1	^{90}Y	1.20E+02	22.0	^{90}Y	1.11E+02	22.2
	^{137m}Ba	1.35E+02	18.3	^{137m}Ba	1.26E+02	20.7	^{137m}Ba	1.17E+02	21.6	^{137m}Ba	1.10E+02	21.9
	^{244}Cm	1.33E+02	18.1	^{244}Cm	1.18E+02	19.5	^{244}Cm	1.05E+02	19.4	^{244}Cm	9.40E+01	18.8
	^{134}Cs	9.79E+01	13.3	^{238}Pu	8.82E+01	14.5	^{238}Pu	8.62E+01	15.8	^{238}Pu	8.41E+01	16.8
	^{238}Pu	9.03E+01	12.3	^{137}Cs	3.60E+01	5.9	^{137}Cs	3.36E+01	6.2	^{137}Cs	3.14E+01	6.3
	^{137}Cs	3.86E+01	5.3	^{134}Cs	3.58E+01	5.9	^{90}Sr	2.51E+01	4.6	^{90}Sr	2.33E+01	4.7
	^{90}Sr	2.90E+01	3.9	^{90}Sr	2.70E+01	4.4	^{241}Am	1.94E+01	3.6	^{241}Am	2.23E+01	4.4
	^{106}Rh	1.68E+01	2.3	^{241}Am	1.60E+01	2.6	^{134}Cs	1.31E+01	2.4	^{154}Eu	8.06E+00	1.6
	^{154}Eu	1.66E+01	2.3	^{154}Eu	1.31E+01	2.1	^{154}Eu	1.03E+01	1.9	^{134}Cs	4.78E+00	1.0
	^{241}Am	1.21E+01	1.6	^{60}Co	3.77E+00	0.6	^{240}Pu	3.30E+00	0.6	^{240}Pu	3.33E+00	0.7
	^{60}Co	5.60E+00	0.8	^{240}Pu	3.28E+00	0.5	^{60}Co	2.54E+00	0.5	^{239}Pu	2.40E+00	0.5
	^{144}Pr	5.58E+00	0.8	^{85}Kr	2.74E+00	0.5	^{239}Pu	2.40E+00	0.4	^{85}Kr	1.86E+00	0.4
	^{85}Kr	3.32E+00	0.5	^{239}Pu	2.40E+00	0.4	^{85}Kr	2.26E+00	0.4	^{60}Co	1.71E+00	0.3

3.3.1.4 Cooling Time Requirements for Regionalized Loading

For each BWR lattice analyzed, the cooling time required to produce a decay heat representative of a typical dry storage cask cell limit using regionalized loading was calculated. ORIGAMI decay calculations were performed over a wide range of cooling times. An exponential function was fit to the data, and cooling time requirements for each decay heat were calculated. The cooling times required to meet the representative decay heat limits are provided in Table 33. The calculated cooling times indicate that LEU+ BWR fuel likely must be stored in basket cells with high decay heat limits to store these assemblies with a reasonable amount of cooling time. The effect of increased burnup and enrichment on the decay heat is generally less impactful for BWR fuel than for PWR; LEU+ BWR fuel has a higher degree of flexibility relative to the loading campaigns of dry storage casks.

Table 33. BWR cooling time requirements for regionalized loading representative decay heat values.

Enrichment (wt %)	**4.3**	**6.6**	**7.9**
Burnup (GWd/MTU)	**55**	**72**	**80**
Decay heat (W)	**Cooling time (years)**	**Cooling time (years)**	**Cooling time (years)**
150	52	77	83
270	30	46	52
370	19	30	35
470	10	17	22
620	5	7	8

3.3.2 Shielding Calculations

Dose rate calculations were performed with SCALE/MAVRIC for a dry storage cask containing BWR fuel with parameters that covered a range of enrichments and cooling times.

3.3.2.1 Shielding Baseline Case

Dose rates for the baseline cases were calculated for the General-89 storage cask type in UNF-ST&DARDS. Dose rate calculations were performed assuming that fuel with one lattice-average enrichment, burnup, and cooling time is uniformly loaded into every cell of the cask. The maximum dose rate at the mid-height on the external cask surface for the baseline case is provided in Table 34. For this analysis, the dose rate at the mid-height on the external cask surface was selected as a representative dose point against which to compare dose rates for LEU+ fuel. Although the calculated dose rates may be higher than would be typically calculated for dry storage casks, a real cask would not be uniformly loaded with such relatively high-burned and low-cooled fuel in this manner. These results only serve to create a baseline against which to compare dose rates for casks loaded with LEU+ fuel.

3.3.2.2 Shielding Extended Enrichment Cases

Dose rates for the LEU+ BWR cases were calculated for the General-89 storage cask type in UNF-ST&DARDS. Dose rate calculations were performed assuming that fuel with one lattice-average enrichment, burnup, and cooling time is uniformly loaded into every cell of the cask. The maximum dose rates at the mid-height on the external cask surface for the LEU+ BWR cases are provided in Table 34. Although dose rates are generally expected to decrease with increased lattice-average enrichment, the results indicate the competing effect of increased burnup on dose rates.

Table 34. LEU+ BWR dose rate results.

Enrichment (wt %)	Burnup (GWd/MTU)	Cooling time (years)	Dose rate (mrem/h)	Relative uncertainty (%)
4.3	55	6.0	8.86E+01	2.06
6.6	72	6.0	1.03E+02	2.23
7.9	80	6.0	1.11E+02	2.27

For each LEU+ BWR assembly, the additional cooling time required to approximately match the baseline dose rate was also calculated. The additional cooling time was calculated by repeating the dose rate calculation at several cooling times, plotting the dose rate as a function of cooling time, fitting a power function to the data, and then using the function to calculate the cooling time required to match the baseline dose rate value. The plots of maximum mid-height surface dose rate vs. cooling time for the 6.6 wt % fuel and the 7.9 wt % fuel are provided in Figure 17 and Figure 18, respectively. The additional cooling times required for each LEU+ BWR fuel to match the baseline dose rate value are provided in Table 35. However, the required additional cooling time may vary depending on the type of overpack (i.e., transportation or storage) and baseline cooling time.

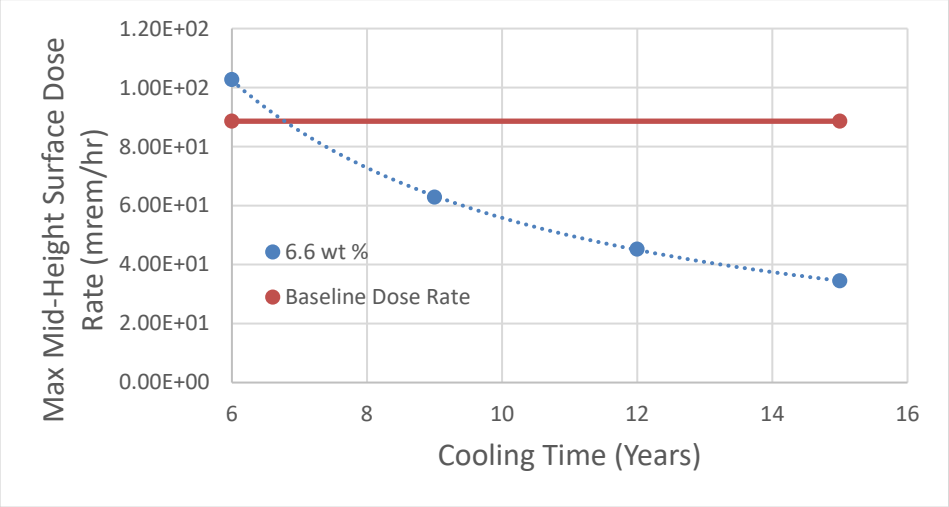

Figure 17. Maximum mid-height surface dose rate vs. cooling time for General-89 loaded with 6.6 wt % BWR fuel.

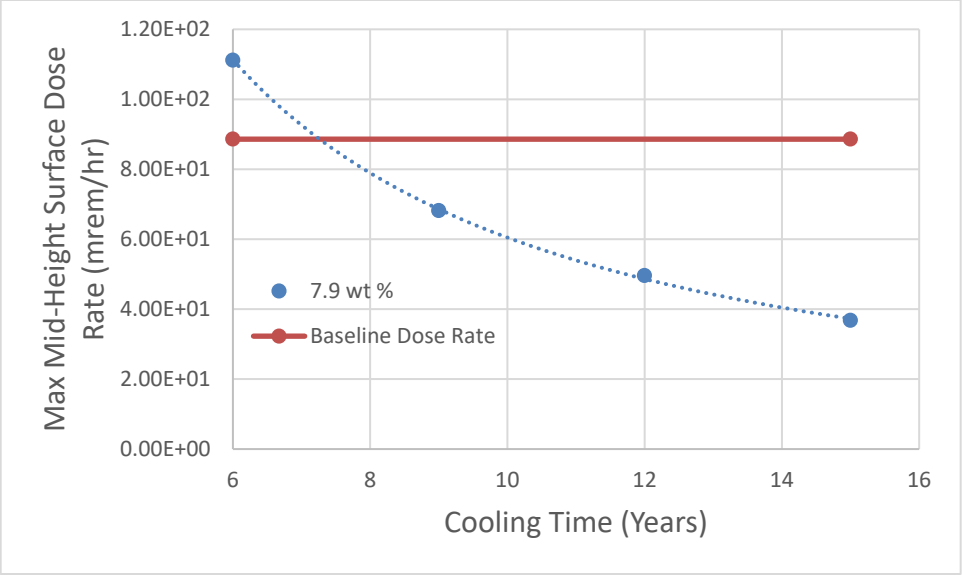

Figure 18. Maximum mid-height surface dose rate vs. cooling time for General-89 loaded with 7.9 wt % BWR fuel.

Table 35. Additional cooling time required for LEU+ BWR fuel to match baseline maximum mid-height surface dose rate.

Enrichment (wt %)	Cooling time (years)	Cooling time delta (years)
6.6	6.78	0.78
7.9	7.26	1.26

3.4 TIME-TO-BOIL ANALYSIS

This section examines the potential effect of extended enrichment and burnup on the time-to-boil of an SFP. Time-to-boil is an important parameter in SFP management because it demonstrates the amount of time available to address the loss of forced cooling. The SFP must be able to accommodate the heat load of a freshly discharged core in the case of an emergency off-load. Because this SFP heat load is dominated by the recently discharged core, this effect was examined by using example fuel management strategies. The minimum time-to-boil after a loss of forced cooling was calculated both for a baseline LEU PWR case and two LEU+ PWR cases. The baseline case consisted of an SFP that contained representative LEU fuel and 1 and 1/3 LEU discharge cores and is discussed more thoroughly in Section 3.4.1. Two LEU+ cases were considered. The first case, representing the first time the LEU+ core is reloaded, consisted of an SFP that contained representative LEU fuel and 1 and 1/3 LEU+ discharge cores. The second case consisted of an SFP that contained representative LEU+ fuel and 1 and 1/3 LEU+ discharge cores. Both cases are discussed more thoroughly in Section 3.4.2.

3.4.1 LEU Discharge Core

Time-to-boil for the baseline case was calculated for a sample SFP containing assemblies from 1 and 1/3 sample discharge LEU cores, as well as assemblies already in the SFP. Decay heats for the assemblies already in the SFP were calculated using assembly discharge data available in UNF-ST&DARDS. The total SFP decay heat was calculated as the sum of all assembly decay heats.

An exposure map and a layout of assembly enrichment and absorber configuration of the southeast quarter of the LEU PWR core used in this analysis adapted from Bae, Mertyurek, and Asgari [10] are provided in Figure 19. The exposure map in this figure is the incremental burnup that will be accumulated during the cycle for each assembly. The fresh (red), once-burned (green), and twice-burned (blue) locations refer to the status of the assembly at the beginning of cycle (BOC). To reduce the number of ORIGAMI depletion and decay calculations required to calculate the decay heat of the core, the assemblies in the core were organized into four groups based on their enrichment, absorber configuration, and cycle-wise burnup, and one discharge calculation was performed for each group. ORIGAMI depletion calculations were performed using libraries from Polaris calculations in Hu, Mertyurek, and Wieselquist [8]. Fuel parameters for each group are provided in Table 36. Thirty days of downtime between cycles were assumed, and 100 h of downtime after shutdown before being loaded into the SFP were assumed. The decay heat of 1 and 1/3 discharge cores was assumed to be the decay heat of one discharge core multiplied by 4/3.

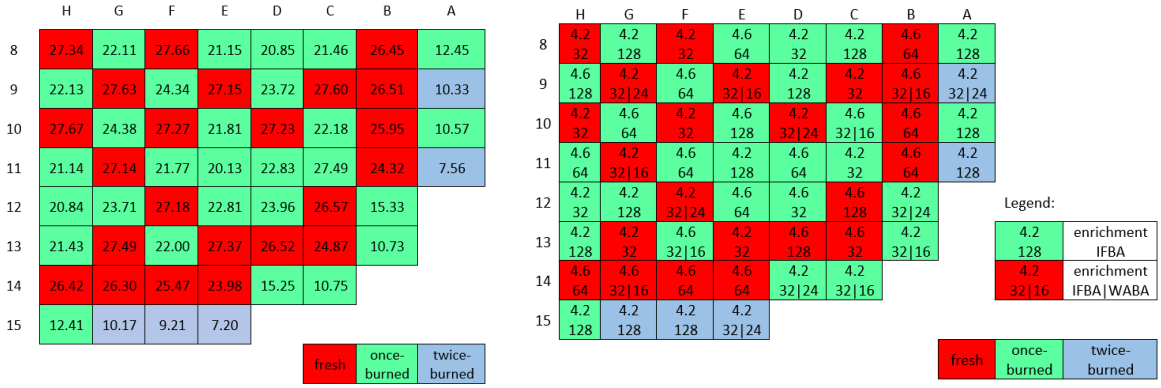

Figure 19. LEU core incremental exposure map (left) and enrichment map (right).

Table 36. Fuel group parameters for LEU discharge core.

	Fresh at BOC	Interior once-burned at BOC	Peripheral once-burned at BOC	Twice-burned at BOC
Enrichment (wt %)	4.2	4.2	4.2	4.2
IFBA/WABA rods	32/0	128/0	32/16	128/0
Burnup (MWd/MTU)	26,543	22,746	12,510	8,894
Cycle length (days)	547.5	547.5	547.5	547.5
Number of assemblies	81	68	24	20
Specific power (MW/MTU)	48.48	41.55	22.85	16.25
Uranium mass (MTU)	42.28	35.50	12.53	10.44

Decay heat calculations were performed for the assemblies already present in the SFP by grouping the inventory by batch enrichment and discharge date and then running ORIGAMI discharge and decay calculations for each group. Each ORIGAMI calculation used the group-total U mass and group-average burnup and assumed each assembly was constantly burned at 30 MW/MTU until the group-average

burnup was achieved. A total of 131 groups with a total U mass of 1,098.28 MTU were used. Cooling time was assumed to be the time between the discharge date and July 1, 2021.

The total SFP decay heat, taken as the sum of the 1 and 1/3 discharge core decay heat and the decay heat of the assemblies already in the SFP was then used to calculate the time-to-boil as described in Abella, Kawata, and Onoue [7]. Assumed properties of the SFP water are provided in Table 37. The calculated time-to-boil for the baseline case is provided in Table 40.

Table 37. Assumed SFP water properties.

SFP water thermal capacity (Btu/°F)	1.0
SFP bulk water temperature (°F)	115
SFP water mass (lb)	3.19E+06

3.4.2 LEU+ Discharge Core

Time-to-boil was calculated for two LEU+ cases. The first case, representing the first time the LEU+ core is reloaded, consisted of an SFP that contained representative LEU fuel and 1 and 1/3 LEU+ discharge cores. In this case, decay heats for the assemblies already in the SFP were identical to those used in the baseline case. The second case consisted of an SFP that contained representative LEU+ fuel and 1 and 1/3 LEU+ discharge cores. This case represented a limiting LEU+ core reload scenario sometime in the future when the entire SFP would contain LEU+ fuel. The approximation of the SFP that contained representative LEU+ fuel is discussed in this section.

An exposure map and a layout of assembly enrichment and absorber configuration of the southeast quarter of the LEU+ PWR core used in this analysis adapted from [10] Bae, Mertyurek, and Asgari are provided in Figure 20. The exposure map in this figure is the incremental burnup that will be accumulated during the cycle for each assembly. The fresh (red), once-burned (green), and twice-burned (blue) locations refer to the status of the assembly at the BOC. To reduce the number of ORIGAMI depletion and decay calculations required to calculate the decay heat of the core, the assemblies in the core were organized into four groups based on their enrichment, absorber configuration, and cycle-wise burnup, and one discharge calculation was performed for each group. ORIGAMI depletion calculations were performed using libraries from Polaris calculations in Hu, Mertyurek, and Wieselquist [8]. Fuel parameters for each group are provided in Table 38. Thirty days of downtime between cycles were assumed, and 100 h of downtime after shutdown before being loaded into the SFP were assumed. The decay heat of 1 and 1/3 discharge cores was assumed to be the decay heat of one discharge core multiplied by 4/3.

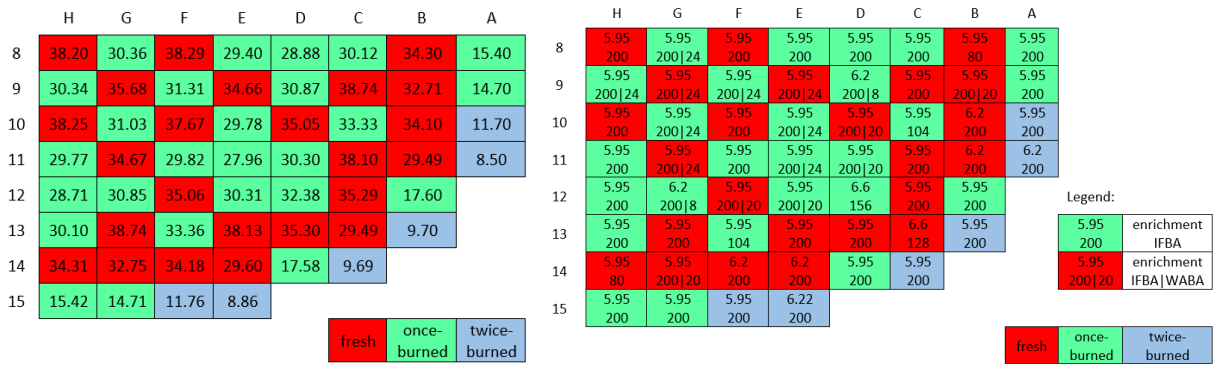

Figure 20. LEU+ core incremental exposure map (left) and enrichment map (right).

Table 38. Fuel group parameters for LEU+ discharge core.

	Fresh at BOC	Interior once-burned at BOC	Peripheral once-burned at BOC	Twice-burned at BOC
Enrichment (wt %)	5.95	5.95	5.95	5.95
IFBA/WABA rods	200/0	200/0	200/0	200/0
Burnup (MWd/MTU)	34,943	30,634	16,000	10,035
Cycle length (days)	730	730	730	730
Number of assemblies	85	64	20	24
Specific power (MW/MTU)	47.87	41.96	21.92	13.75
Uranium mass (MTU)	44.37	33.41	10.44	12.53

For the case with 1 and 1/3 LEU+ discharge cores and an SFP that contained representative LEU fuel, the decay heat of the assemblies already present in the SFP was calculated, as described in the previous section.

For the case with 1 and 1/3 LEU+ discharge cores and an SFP that contained representative LEU+ fuel, the entire SFP was assumed to contain LEU+ fuel. The decay heat was calculated by applying a uniform burnup multiplier to all the fuel in the representative LEU SFP to approximate an SFP loaded with representative LEU+ fuel. This burnup multiplier was chosen to be 1.35, which approximately represents the ratio of average LEU+ fuel burnup (75 GWd/MTU) to average LEU fuel burnup (55 GWd/MTU). Using Polaris calculations from Hu, Mertyurek, and Wieselquist [8], ORIGAMI was used to calculate the decay heat of various LEU and LEU+ PWR fuel assemblies. These decay heat results at sample enrichments are provided in Table 39 and demonstrate that, at a given burnup, lower enrichment generally results in higher decay heat over the cooling time range analyzed. The background SFP decay heat was approximately one order of magnitude lower than the discharge core decay heat; therefore, this assumption has very little effect on the calculated time-to-boil. This work preferred this type of bounding estimate for the decay heat in the LEU+ SFP for two reasons. First, SFP management strategies may change for LEU+ fuel because of longer cycle lengths. Second, plants changing from LEU to LEU+ will still have a significant amount of LEU fuel in the SFP, and it may take considerable time for the SFP to become predominantly populated by LEU+ fuel. The effect of increasing burnup for a fixed enrichment on the nuclide inventory and decay heat of a range of PWR assemblies is further investigated in Appendix A.

Table 39. Decay heat of LEU fuel assembly with increased burnup compared to LEU+ fuel.

Enrichment (wt %)	4.6	4.6	6.6	Decay heat increase (%)
Burnup (GWd/MTU)	52	72	72	
IFBAs/WABAs	128	128	128	
Cooling time (years)	**Decay heat (W)**			
0	1.07E+06	1.06E+06	1.07E+06	-1.36
1	6.17E+03	7.96E+03	7.36E+03	8.15
5	1.29E+03	2.00E+03	1.82E+03	9.85
10	8.35E+02	1.32E+03	1.22E+03	7.87
20	6.46E+02	9.96E+02	9.43E+02	5.65
30	5.37E+02	8.11E+02	7.80E+02	3.92
40	4.53E+02	6.71E+02	6.55E+02	2.46

In both cases, the total SFP decay heat, taken as the sum of the discharge core decay heat and the decay heat of the assemblies already in the SFP, was then used to calculate the time-to-boil, as described in Abella, Kawata, and Onoue [7]. Assumed properties of the SFP water were identical to those used in the baseline case. The calculated time-to-boil for the LEU+ cases is provided in Table 40. For both LEU+ cases, the time-to-boil was only slightly shorter than that of the SFP that contained the LEU discharge

core and representative LEU fuel. For all cases, the decay heat from the fuel in the SFP was generally smaller than the decay heat from the discharge core.

Table 40. Time-to-boil results.

	Baseline (LEU core and LEU SFP)	LEU+ core and LEU SFP	LEU+ core and LEU+ SFP
1 and 1/3 discharge core decay heat (W)	1.79E+07	1.84E+07	1.84E+07
SFP decay heat (W)	1.94E+06	1.94E+06	2.93E+06
Total SFP decay heat (W)	1.98E+07	2.03E+07	2.13E+07
Time-to-boil (h)	4.58	4.46	4.26

4. CONCLUSIONS

This work investigated the effect of loading LEU+ fuel with extended enrichment and burnup on the thermal and shielding performance of current dry storage cask systems. Generally, loading LEU+ fuel with extended enrichment and burnup into dry storage casks requires additional cooling time to achieve decay heat and dose rates of standard LEU fuel. Given the three variables of enrichment, burnup, and cooling time, the following behaviors are generally expected.

- Increased enrichment (i.e., holding burnup and cooling time constant) decreases dose rates and decay heat.
- Increased burnup (i.e., holding enrichment and cooling time constant) increases dose rates and decay heat.
- Increased cooling time (i.e., holding enrichment and burnup constant) decreases dose rates and decay heat.

This information can help indicate whether an existing LEU limit will be bounding for LEU+. For example, if a transportation limit is based on decay heat and dose rates for 5% enriched fuel at 75 GWd/MTU, then that same transportation limit would also hold conservatively for LEU+ at 75 GWd/MTU. The combinations of burnup and enrichment analyzed in this report are intended to be realistic and include both increased enrichment and burnup, as necessary, to achieve longer cycle lengths and/or reduced batch loading for current LWRs. The isolated effects of increasing burnup, enrichment, or cooling time are further studied in Hall et al. [14].

4.1 PWR DRY STORAGE ANALYSIS

The decay heat of one 17 × 17 PWR assembly increased with extended enrichment and burnup. PCT for a General-37 cask uniformly loaded with 17 × 17 LEU+ PWR fuel also increased with extended enrichment and burnup. For the LEU+ PWR fuel enrichments analyzed, between 5.82 and 8.87 years of additional cooling time were required to match the PCT calculated for a baseline LEU PWR case with 6 years cooling. This difference may decrease with a longer baseline cooling time for LEU, but this depends on the radionuclides dominating the total decay heat at a given cooling time. The decay heat and PCT of the LEU and LEU+ PWR enrichments analyzed were shown not to depend strongly on the absorber amount and configuration in the fuel lattice. Generally, for all LEU and LEU+ PWR enrichments analyzed, the same radionuclides contributed the most to the assembly decay heat and did not depend strongly on the absorber amount and configuration in the fuel lattice.

Cooling times required to produce a decay heat representative of a typical dry cask storage cell limit using regionalized loading were calculated for LEU+ PWR fuel. The calculated cooling times indicate that

LEU+ PWR fuel likely must be stored in basket cells with relatively high decay heat limits to store these assemblies with a reasonable amount of cooling time.

The maximum mid-height surface dose rate for a General-37 cask uniformly loaded with LEU+ PWR fuel increased by approximately 130% with extended enrichment and burnup. For the LEU+ PWR fuel enrichments and cooling time analyzed, between 1.37 and 1.51 years of additional cooling time were required to match the dose rate calculated for a baseline LEU case with 6 years cooling. For the LEU and LEU+ PWR fuel analyzed, the maximum mid-height surface dose rate did not depend strongly on the absorber amount and configuration in the fuel lattice.

4.2 BWR DRY STORAGE ANALYSIS

The decay heat of one 10 × 10 BWR assembly increased with extended enrichment and burnup. PCT for a General-68 cask uniformly loaded with 10 × 10 LEU+ BWR fuel also increased with extended enrichment and burnup. For the LEU+ BWR fuel lattice-average enrichments analyzed, between 5.56 and 9.36 years of additional cooling time were required to match the PCT calculated for a baseline LEU BWR case with 6 years cooling. Naturally, this difference will decrease with a longer baseline cooling time for LEU. Generally, for all LEU and LEU+ BWR enrichments analyzed, the same nuclides contributed the most to the assembly decay heat and did not depend strongly on the lattice-average enrichment or the Gd concentration of the fuel.

Cooling times required to produce a decay heat representative of a typical dry cask storage cell limit using regionalized loading were calculated for LEU+ BWR fuel. The calculated cooling times indicate that LEU+ BWR fuel likely must be stored in basket cells with relatively high decay heat limits to store these assemblies with a reasonable amount of cooling time, but increased burnup and enrichment generally affect decay heat less for BWR fuel than for PWR.

The maximum mid-height surface dose rate for a General-89 cask uniformly loaded with LEU+ BWR fuel increased by approximately 120% with extended enrichment and burnup. For the LEU+ BWR fuel lattice-average enrichments and cooling time analyzed, between 0.78 and 1.26 years of additional cooling time were required to match the dose rate calculated for a baseline LEU case.

4.3 TIME-TO-BOIL ANALYSIS

The time-to-boil of an SFP loaded with representative LEU fuel and 1 and 1/3 LEU discharge cores was calculated and compared with that of two LEU+ cases. The LEU+ cases represented the first “transition” LEU+ core reload and a limiting “equilibrium” LEU+ core reload, assuming the SFP is full of LEU+ discharged fuel. The calculated time-to-boil for the LEU+ cases were only slightly shorter than the time-to-boil for the SFP that contained the LEU core. At short cooling times, the decay heats of the LEU and LEU+ cores were similar and thus the effect on time-to-boil was minimal compared with the effect of LEU+ on dry storage cask performance. Changes to SFP management may be needed because of the additional cooling time required for LEU+ fuel to be loaded into dry storage casks, but the longer cycle length achievable for LEU+ fuel may help offset these changes.

5. REFERENCES

[1] W. A. Wieselquist, R. A. Lefebvre, and M. A. Jessee, Eds., *SCALE Code System,* ORNL/TM-2005/39, Version 6.2.4, Oak Ridge National Laboratory, Oak Ridge, TN (2020).

[2] T. E. Michener, D. R. Rector, J. M. Cuta, and H. E. Adkins, Jr. 2015. *COBRA-SFS: A Thermal Hydraulic Analysis Code for Spent Fuel Storage and Transportation Casks Cycle 4*. PNNL-24841, Richland: Pacific Northwest National Laboratory.

[3] R. A. Lefebvre, P. Miller, J. M. Scaglione, K. Banerjee, J. L. Peterson, G. Radulescu, K. R. Robb, A. B. Thompson, H. Liljenfeldt & J. P. Lefebvre (2017). Development of Streamlined Nuclear Safety Analysis Tool for Spent Nuclear Fuel Applications, Nuclear Technology, 199:3, 227-244, DOI: 10.1080/00295450.2017.1314747.

[4] T. E. Michener, D. R. Rector, and J. M. Cuta. 2017. "Validation of COBRA-SFS with Measured Temperature Data from Spent-Fuel Storage Casks." *Nuclear Technology* 199, no. 3: 350–368. DOI: 10.1080/00295450.2017.1327253.

[5] D. R. Rector. 1987. *RADGEN: A Radiation Exchange Factor Generator for Rod Bundles*. PNNL-6342, Richland: Pacific Northwest National Laboratory.

[6] ANSI-6.1.1 Working Group, M.E. Battat (Chairman), "American National Standard Neutron and Gamma-Ray Flux-to-Dose Rate Factors," ANSI/ANS-6.1.1-1977 (N666), American Nuclear Society, LaGrange Park, Illinois (1977).

[7] L. Abella, N. Kawata, and M. Onoue. 2009. *Thermal-Hydraulic Analysis for US-APWR Spent Fuel Racks*. MUAP-09014NP-R0, Mitsubishi Heavy Industries LTD.

[8] J. Hu, U. Mertyurek, and W. Wieselquist. 2022. *Assessment of the Polaris/PARCS Two-Step Approach for Reactor Core Modeling with Extended Enrichment and High Burnup LWR Fuels. Vol. I: PWR*. ORNL/TM-2022/1831, Oak Ridge: Oak Ridge National Laboratory.

[9] J. Hu, U. Mertyurek, and W. Wieselquist. 2022. *Assessment of the Polaris/PARCS Two-Step Approach for Reactor Core Modeling with Extended Enrichment and High Burnup LWR Fuel. Vol. II: BWR.* ORNL/TM-2022/2444, Oak Ridge: Oak Ridge National Laboratory.

[10] J. W. Bae, U. Mertyurek, and M. Asgari. 2022. *Light Water Reactor LEU+ Lattice Optimization*. ORNL/TM-2021/2366, Oak Ridge: Oak Ridge National Laboratory.

[11] *Spent Fuel Project Office, Interim Staff Guidance – 11*. 2003. Revision 3. "Cladding Considerations for the Transportation and Storage of Spent Fuel."

[12] 10 CFR Part 72. 2017. "Licensing Requirements for the Independent Storage of Spent Nuclear Fuel, High-Level Radioactive Waste, and Reactor-Related Greater Than Class C Waste." *Code of Federal Regulations*, Title 10, *Energy*, Part 72, Washington, DC.

[13] B. L. Broadhead, *Recommendations for Shielding Evaluations for Transport and Storage Packages,* NUREG/CR-6802 (ORNL/TM-2002/31), U.S. Nuclear Regulatory Commission, Oak Ridge National Laboratory (2003).

[14] R. Hall, R. Cumberland, R. Sweet, and W. Wieselquist. 2021. *Isotopic and Fuel Lattice Parameter Trends in Extended Enrichment and Higher Burnup LWR Fuel.* ORNL/TM-2020/1833, Oak Ridge: Oak Ridge National Laboratory.

[15] J. Hu, I. Gauld, A. Worrall, H. Liljenfeldt, S. Park, A. Sjoland, S. Ahn, and H. Kim. *Spent Fuel Modeling and Simulation Using ORIGAMI for Advanced NDA Instrument Testing.* ANS MC2015 - Joint International Conference on Mathematics and Computation (2015).

APPENDIX A. NUCLIDE INVENTORIES AND DECAY HEATS OF LEU AND LEU+ FUEL

APPENDIX A. NUCLIDE INVENTORIES AND DECAY HEATS OF LEU AND LEU+ FUEL

In this appendix, nuclide inventories and decay heats for several LEU and LEU+ PWR and BWR fuel assemblies used in [8] (PWR) and [9] (BWR) are provided. Nuclide inventories may be of interest in the context of environmental considerations.

For each fuel assembly analyzed, Polaris depletion results were used as input to ORIGEN decay calculations to generate the data contained in this appendix. The Polaris depletion calculations assumed a constant power history. Nuclide inventories and fuel parameters for the analyzed fuel lattices are provided in the accompanying file "ORNL-TM-2022-1841_AppendixA.xlsx".

PWR results are provided for each lattice at both 52 GWd/MTU and 72 GWd/MTU assembly burnups. For each PWR assembly, the peak rod burnup is also provided. The PWR peak rod burnup was obtained by multiplying the assembly burnup by a burnup-peaking factor of 1.07 (for 52 GWd/MTU assemblies) or 1.08 (for 72 GWd/MTU assemblies). These burnup-peaking factors were calculated by dividing the peak pin burnup by the assembly-average burnup for representative LEU and LEU+ PWR assemblies analyzed in [8]. These factors are similar to the burnup-peaking factor of 1.07 for the 17 × 17 PWR5 assembly analyzed in [15].

BWR results are provided for each lattice at both 52 GWd/MTU and 72 GWd/MTU assembly burnups. For each BWR assembly, the peak rod burnup is also provided. The BWR peak rod burnup was assumed to be 1.09 for LEU assemblies and 1.11 for LEU+ assemblies based on results in [9].

Decay heats for these PWR and BWR assemblies over a range of cooling times (also provided in the attached file "Appendix_A_Summary.xlsx") are provided in Tables A-1 and A-2, respectively. For all lattices analyzed, increasing the burnup while keeping the enrichment and cooling time constant resulted in higher decay heat. These results support the use of the burnup multiplier to approximate the decay heat of the LEU+ SFP in Section 3.4.2.

Table A-1. Summary of LEU and LEU+ PWR decay heats.

File Name	Enrich. (wt.%)	IFBA Count (-)	WABA Count (-)	Burnup (GWD/MTU)	Burnup-Peaking Factor	Peak Rod Burnup (GWD/MTU)	Specific Power (W/kg)	Initial Mass (MTU)	Total Decay Heat (W) as a function of Cooling Time (years)						
									0	1	5	10	20	30	40
6.6_i156-CR0-MDC-MPC-MTF_52GWD_40SP.out	6.60	156	0	52	1.07	55.64	40	0.44	1.082E+06	5727	1200	800	626	522	441
6.2_i200-CR0-MDC-MPC-MTF_52GWD_40SP.out	6.20	200	0	52	1.07	55.64	40	0.44	1.078E+06	5772	1204	799	624	520	439
6.6_i128-CR0-MDC-MPC-MTF_52GWD_40SP.out	6.60	128	0	52	1.07	55.64	40	0.44	1.083E+06	5743	1206	803	628	525	444
6.2_i200_w08-CR0-MDC-MPC-MTF_52GWD_40SP.out	6.20	200	8	52	1.07	55.64	40	0.44	1.078E+06	5788	1208	802	627	523	442
5.95_i80-CR0-MDC-MPC-MTF_52GWD_40SP.out	5.95	80	0	52	1.07	55.64	40	0.44	1.078E+06	5889	1236	817	638	533	451
5.95_i104-CR0-MDC-MPC-MTF_52GWD_40SP.out	5.95	104	0	52	1.07	55.64	40	0.44	1.080E+06	5938	1252	828	647	542	460
5.95_i200-CR0-MDC-MPC-MTF_52GWD_40SP.out	5.95	200	0	52	1.07	55.64	40	0.44	1.080E+06	5946	1253	829	649	544	462
5.95_i200_w20-CR0-MDC-MPC-MTF_52GWD_40SP.out	5.95	200	20	52	1.07	55.64	40	0.44	1.080E+06	5989	1265	838	657	552	470
5.95_i200_w24-CR0-MDC-MPC-MTF_52GWD_40SP.out	5.95	200	24	52	1.07	55.64	40	0.44	1.080E+06	5997	1267	840	659	554	472
4.6_i128-CR0-MDC-MPC-MTF_52GWD_40SP.out	4.60	128	0	52	1.07	55.64	40	0.44	1.065E+06	6172	1287	835	646	537	453
4.6_i64-CR0-MDC-MPC-MTF_52GWD_40SP.out	4.60	64	0	52	1.07	55.64	40	0.44	1.067E+06	6208	1300	844	654	544	460
4.2_i128-CR0-MDC-MPC-MTF_52GWD_40SP.out	4.20	128	0	52	1.07	55.64	40	0.44	1.061E+06	6283	1310	845	651	541	455
4.6_i32-CR0-MDC-MPC-MTF_52GWD_40SP.out	4.60	32	0	52	1.07	55.64	40	0.44	1.069E+06	6244	1313	853	661	552	467
4.6_i32_w16-CR0-MDC-MPC-MTF_52GWD_40SP.out	4.60	32	16	52	1.07	55.64	40	0.44	1.069E+06	6276	1322	860	668	558	473
4.2_64-CR0-MDC-MPC-MTF_52GWD_40SP.out	4.20	64	0	52	1.07	55.64	40	0.44	1.063E+06	6319	1324	855	659	548	462
4.2_i32-CR0-MDC-MPC-MTF_52GWD_40SP.out	4.20	32	0	52	1.07	55.64	40	0.44	1.065E+06	6355	1337	864	667	555	469
4.2_i32_w16-CR0-MDC-MPC-MTF_52GWD_40SP.out	4.20	32	16	52	1.07	55.64	40	0.44	1.066E+06	6385	1346	871	674	562	476
4.2_i32_w24-CR0-MDC-MPC-MTF_52GWD_40SP.out	4.20	32	24	52	1.07	55.64	40	0.44	1.066E+06	6401	1351	875	677	565	479
6.6_i156-CR0-MDC-MPC-MTF_72GWD_40SP.out	6.60	156	0	72	1.08	77.76	40	0.44	1.069E+06	7335	1811	1217	938	775	650
6.6_i128-CR0-MDC-MPC-MTF_72GWD_40SP.out	6.60	128	0	72	1.08	77.76	40	0.44	1.070E+06	7358	1820	1224	943	780	655
6.2_i200-CR0-MDC-MPC-MTF_72GWD_40SP.out	6.20	200	0	72	1.08	77.76	40	0.44	1.065E+06	7406	1824	1221	937	772	646
6.2_i200_w08-CR0-MDC-MPC-MTF_72GWD_40SP.out	6.20	200	8	72	1.08	77.76	40	0.44	1.065E+06	7426	1831	1227	942	777	650
5.95_i80-CR0-MDC-MPC-MTF_72GWD_40SP.out	5.95	80	0	72	1.08	77.76	40	0.44	1.066E+06	7575	1884	1260	966	797	668
5.95_i104-CR0-MDC-MPC-MTF_72GWD_40SP.out	5.95	104	0	72	1.08	77.76	40	0.44	1.069E+06	7639	1908	1279	983	813	683
5.95_i200-CR0-MDC-MPC-MTF_72GWD_40SP.out	5.95	200	0	72	1.08	77.76	40	0.44	1.069E+06	7643	1910	1281	985	815	685
5.95_i200_w20-CR0-MDC-MPC-MTF_72GWD_40SP.out	5.95	200	20	72	1.08	77.76	40	0.44	1.070E+06	7697	1928	1296	999	828	697
5.95_i200_w24-CR0-MDC-MPC-MTF_72GWD_40SP.out	5.95	200	24	72	1.08	77.76	40	0.44	1.070E+06	7709	1932	1299	1002	831	700
4.6_i128-CR0-MDC-MPC-MTF_72GWD_40SP.out	4.60	128	0	72	1.08	77.76	40	0.44	1.055E+06	7958	1999	1320	996	811	671
4.6_i64-CR0-MDC-MPC-MTF_72GWD_40SP.out	4.60	64	0	72	1.08	77.76	40	0.44	1.058E+06	8007	2019	1335	1009	823	682
4.6_i32-CR0-MDC-MPC-MTF_72GWD_40SP.out	4.60	32	0	72	1.08	77.76	40	0.44	1.060E+06	8053	2037	1350	1022	835	694
4.2_i128-CR0-MDC-MPC-MTF_72GWD_40SP.out	4.20	128	0	72	1.08	77.76	40	0.44	1.053E+06	8093	2046	1348	1012	819	675
4.6_i32_w16-CR0-MDC-MPC-MTF_72GWD_40SP.out	4.60	32	16	72	1.08	77.76	40	0.44	1.061E+06	8091	2050	1361	1033	845	703
4.2_64-CR0-MDC-MPC-MTF_72GWD_40SP.out	4.20	64	0	72	1.08	77.76	40	0.44	1.055E+06	8140	2065	1363	1025	831	686
4.2_i32-CR0-MDC-MPC-MTF_72GWD_40SP.out	4.20	32	0	72	1.08	77.76	40	0.44	1.057E+06	8186	2083	1377	1037	843	698
4.2_i32_w16-CR0-MDC-MPC-MTF_72GWD_40SP.out	4.20	32	16	72	1.08	77.76	40	0.44	1.058E+06	8222	2096	1388	1047	853	707
4.2_i32_w24-CR0-MDC-MPC-MTF_72GWD_40SP.out	4.20	32	24	72	1.08	77.76	40	0.44	1.059E+06	8241	2103	1394	1053	858	712

Table A-2. Summary of LEU and LEU+ BWR decay heats.

File Name	Enrich. (wt.%)	Burnup (GWD/MTU)	Burnup-Peaking Factor	Peak Rod Burnup (GWD/MTU)	Specific Power (W/kg)	Initial Mass (MTU)	Total Decay Heat (W) as a function of Cooling Time (years)						
							0	1	5	10	20	30	40
G4610G14-e7.9_b52GWD.out	7.9	52	1.09	56.68	25	0.179	275860	1666	432	308	243	202	171
G4610G14-e6.6_b52GWD.out	6.6	52	1.09	56.68	25	0.179	274060	1725	444	313	247	205	173
G4610G14-e4.3_b52GWD.out	4.3	52	1.09	56.68	25	0.179	269630	1884	478	329	255	211	177
G4610G14-e7.9_b72GWD.out	7.9	72	1.11	79.92	25	0.179	272780	2113	638	460	360	298	250
G4610G14-e6.6_b72GWD.out	6.6	72	1.11	79.92	25	0.179	270860	2207	665	475	369	304	254
G4610G14-e4.3_b72GWD.out	4.3	72	1.11	79.92	25	0.179	267330	2422	739	517	392	317	261